Two novel fungal negative-strand RNA viruses related to mymonaviruses and phenuiviruses in the shiitake mushroom (*Lentinula edodes*)

Yu-Hsin Lin[a,1,2], Miki Fujita[a,1], Sotaro Chiba[b,c], Kiwamu Hyodo[a], Ida Bagus Andika[a, 3], Nobuhiro Suzuki[a], Hideki Kondo[a,*]

[a] Institute of Plant Science and Resources (IPSR), Okayama University, Kurashiki 710-0046, Japan

[b] Graduate School of Bioagricultural Sciences, Nagoya University, Nagoya 464-8601, Japan;

[c] Asian Satellite Campuses Institute, Nagoya University, Nagoya 464-8601, Japan

[1] These authors contributed equally to this work.

[2] Present address: Hayashibara Co., Ltd., Naka-ku, Okayama 702-8002, Japan.

[3] Present address: College of Plant Health and Medicine, Qingdao Agricultural University, Qingdao 266109, China

***Corresponding author**
Hideki Kondo
Institute of Plant Science and Resources (IPSR), Okayama University,
Kurashiki 710-0046, Japan
E-mail: hkondo@okayama.u-ac.jp
Tel. +81(86) 434-1232 / Fax. +81(86) 434-1232

The GenBank/EMBL/DDBJ accession numbers for the viral genome sequences reported in this paper are LC466007 (LeNSRV1), LC466008 (LeNSRV2 RNA1) and LC466009 (LeNSRV2 RNA2)

MS information:
Abstract, 149 words; Main Text, 6864 words; Figures, 5; table, 1; Supplemental tables, 2; Supplemental figures, 6.

Abstract

There is still limited information on the diversity of (–)ssRNA viruses that infect fungi. Here, we have discovered two novel (–)ssRNA mycoviruses in the shiitake mushroom (*Lentinula edodes*). The first virus has a monopartite RNA genome and relates to that of mymonaviruses (*Mononegavirales*), especially to Hubei rhabdo-like virus 4 from arthropods and thus designated as Lentinula edodes negative-strand RNA virus 1. The second virus has a putative bipartite RNA genome and is related to the recently discovered bipartite or tripartite phenui-like viruses (*Bunyavirales*), associated with plants and ticks, and designated as Lentinula edodes negative-strand RNA virus 2 (LeNSRV2). LeNSRV2 is likely the first segmented (–)ssRNA virus known to infect fungi. Its smaller RNA segment encodes a putative nucleocapsid and a plant MP-like protein, using a potential ambisense coding strategy. These findings enhance our understanding of the diversity, evolution and spread of (–)ssRNA viruses in fungi.

Keywords

Lentinula edodes; Shitake Mushroom; High-throughput sequencing; Negative-strand RNA virus; *Mymonaviridae*; *Phenuiviridae*; Bipartite genome; Ambisense; Endogenous virus element; Evolution

Highlights

► Two novel fungal (–)ssRNA viruses, LeNSRV1 and LeNSRV2, were discovered in Shiitake mushroom through deep sequencing.

► LeNSRV1 is the first example of a mymonavirus infecting basidiomycetes and has the largest genome among known mymonaviruses.

► LeNSRV2 is the first example of a fungal (–)ssRNA virus with a segmented genome and is related to recently discovered plant phenui-like viruses, having a potential ambisense transcription strategy.

► These findings enhance our understanding of the diversity, evolution, and spread of fungal (–)ssRNA viruses.

1. Introduction

Negative-strand (−) single-stranded RNA (ssRNA) viruses include many important pathogens of humans (e.g, Ebola, Rabies, Rift Valley fever, and influenza A viruses), as well as livestock (e.g, vesicular stomatitis Indiana and Peste-des-petits-ruminants viruses) and plants (e.g, tomato spotted wilt and rice stripe viruses) (King et al., 2011; Kormelink et al., 2011). The most of the (−)ssRNA viruses are divided into two large viral lineages based on whether their RNA genomes are non-segmented or segmented (Ruigrok et al., 2011). The nonsegmented (−)ssRNA viruses as well as some bipartite (−)ssRNA viruses, i.e., members of the genera *Dichorhavirus* and *Varicosavirus*) belong to the single order *Mononegavirales,* which currently comprises 11 families, such as *Rhabdoviridae, Paramyxoviridae* and *Filoviridae* (Amarasinghe et al., 2018; Walker et al., 2018). In contrast, most of the segmented (−)ssRNA viruses belong to the order *Bunyavirales,* which contains 12 families, such as *Arenaviridae* (two or three segments), *Peribunyaviridae* (three segments), and *Phenuiviridae* (three segments except for tenuiviruses with four to six segments) (Maes et al., 2018), and families such as *Orthomyxoviridae* (six to eight segments), and *Aspiviridae* (formerly *Ophioviridae*, three or four segments) (García et al., 2018; King et al., 2011). Recently, metaviromic (metatranscriptomic) analyses of invertebrate samples (mainly arthropods) have greatly expanded the diversity of (−)ssRNA viruses and led to the discovery of novel groups, such as the *Chuviridae, Qinviridae* and *Yueviridae* families, in addition to aspiviruses (ophioviruses), all of which have been placed in the major phylogenetic gap between the two large groups of (−)ssRNA viruses (Kuhn et al., 2019; Li et al., 2015; Shi et al., 2016; Wolf et al., 2018).

Fungal viruses are widespread throughout the major taxonomic groups of fungi, including yeasts, mushrooms, plant-, insect-, and human-pathogenic fungi (Ghabrial et al., 2015; Pearson et al., 2009; Quesada-Moraga et al., 2014). Currently, 18 families and one genus of fungal viruses have been officially ratified by the International Committee for the Taxonomy of Viruses (ICTV) (https://talk.ictvonline.org/taxonomy/) (Kotta-Loizou and Coutts, 2017). Most fungal viruses have either double-stranded RNA (dsRNA) or positive-strand (+)ssRNA genomes, however, recent reports have expanded our knowledge of fungal virus diversity by findings of fungal viruses with monopartite (−)ssRNA (family *Mymonaviridae*, in the order *Mononegavirales*) and

ssDNA genomes (geminivirus-related DNA mycoviruses) (Kondo et al., 2013a; Liu et al., 2014; Yu et al., 2010). Furthermore, recent large-scale meta-transcriptomic analyses of plant pathogenic fungi have also uncovered the presence of several fungal (−)ssRNA viruses, including mymonaviruses (Hao et al., 2018; Marzano and Domier, 2016; Marzano et al., 2016; Mu et al., 2018; Wang et al., 2018b) and other fungal (−)ssRNA viruses related to bi- and tripartite (−)ssRNA viruses, such as phenuiviruses and peribunyaviruses (in the order *Bunyavirales*), and a group of multipartite (−)ssRNA viruses (ophioviruses) (Donaire et al., 2016; Marzano et al., 2016; Osaki et al., 2016). However, there has been no direct evidence regarding the presence of fungal (−)ssRNA viruses with bi- or multipartite genomes.

Most fungal viruses seem to have no significant effect on their fungal hosts, whereas some mycoviruses infecting plant-pathogenic fungi can reduce the growth, virulence (termed "hypovirulence") or fungicide resistance of their hosts, therefore, many studies have so far focused on the fungal viruses as potential for biological control agents against fungal diseases (Kondo et al., 2013b; Niu et al., 2018; Nuss, 2005; Xie and Jiang, 2014). Interestingly, some viruses can enhance the fungal virulence (termed "hypervirulence") of plant- and human-pathogenic fungi (Ahn and Lee, 2001; Lau et al., 2018; Ozkan and Coutts, 2015). Fungal viruses are also important in mushroom cultivations because they are the causal viral agents for certain mushroom diseases, and are associated with economically important mushroom diseases of several fungal species, including white-button mushroom (*Agaricus bisporus*), enokitake mushroom (*Flammulina velutipes*), shiitake mushroom (*Lentinula edodes*), oyster mushrooms (*Pleurotus eryngii* and *P. ostreatus*) (Magae, 2012; Magae and Sunagawa, 2010; Qiu et al., 2010; Revill et al., 1994; Ro et al., 2007; Ro et al., 2006) . In addition, many others have also been identified from asymptomatic edible mushrooms (Ghabrial et al., 2015; Komatsu et al., 2019; Sahin and Akata, 2018 and references therein; Wang et al., 2018a).

Shiitake is the second most important edible mushrooms among the industrially cultivated species, with that over 1,321,000 tons being produced in the southeast Asian countries (Miles and Chang, 2004). In the 1970s, many fungal virus-like agents with different particle morphologies and dsRNA profiles have been discovered in Shiitake (Rytter et al., 1991; Ushiyama, 1979 and references therein). The presence of two fungal dsRNA viruses, Lentinula edodes mycovirus HKB (LeV-HKB) and Lentinula edodes partitivirus 1 (LePV1), belonging to the proposed genus "Phlegivirus" and the genus *Betapartitivirus* (in the family *Partitiviridae*), respectively, has been

reported in some diseased shiitake strains (Guo et al., 2017; Kim et al., 2013; Magae, 2012; Won et al., 2013). However, details of other shiitake-infecting viruses, especially fungal (−)ssRNA viruses, and their diversity is still limited.

In this study, deep sequencing was used to investigate the virome of a single strain of shiitake, which is derived from the fruiting body grows on the hardwood logs in Japan. As a result, a multiple viral infection was identified, including novel fungal (−)ssRNA viruses related to mymonaviruses and phenuiviruses. Sequence comparisons and phylogenetic analyses revealed that these two (−)ssRNA viruses were considered to be unreported fungal viruses, and therefore, they were designated as Lentinula edodes negative-strand RNA virus 1 (LeNSRV1) and Lentinula edodes negative-strand RNA virus 2 (LeNSRV2). The genome information of two novel fungal (−)ssRNA viruses provides interesting new insight into the diversity, evolution and spread of fungal (−)ssRNA viruses. In particular for LeNSRV2, being likely the first example of a fungal virus with a segmented genome that uses an ambisense transcription strategy.

2. Results and discussions

2.1. Virome analysis of a single *Lentinula edodes* strain, HG3

We attempted to search for (–)ssRNA virus-like sequences in the fungal NCBI database using a BlastP search with a query for the large protein L (replicase, containing RdRP domain) of known fungal (–)ssRNA viruses as a query. Blast search identified a partial sequence of a previously unreported mymona-like virus sequence (1.6 kb, accession no. JQ687141) from shiitake in South Korea (data not shown). Using a primer set specific for this sequence, we conducted RT-PCR analysis on commercially available shiitake fruiting bodies. RT-PCR analysis confirmed the infection of this virus-like agent, together with a known fungal dsRNA virus (LeV-HKB), in a fruiting body sample (referred to as HG3) that grows on the hardwood logs in Hyogo Prefecture, Japan; but it was not found in other examined shiitake fruiting bodies that are grown on artificial sawdust media (mushroom bed) in Okayama and Nagasaki Prefectures (Fig. 1A and B and data not shown). To further characterize the genomic structure of the novel mymona-like virus and other possibly hidden fungal viruses, we conducted high-throughput sequencing of the total RNA (depleted ribosomal RNA) sample from the HG3 mycelia (Fig. 1C) using the Illumina HiSeq 4000 platform.

A total of 111,394,862 reads were obtained from the deep sequencing analysis. The assembled 7,630 contigs (>1,000 nt) were subsequently subjected to local tBlastN analysis against NCBI virus Refseq records. We found the presence of at least 13 virus-like contigs with a size of 2,773–11,566 nt and average coverage of 1,184–183,332 reads (YL, MF, and HK unpublished results). These virus-like contigs represent nine putative fungal viruses and two their variants (see below) and seem to cover most of the viral genomic regions. The largest contig was derived from a previously identified mymona-like virus sequence (contig no. 585, 11566 nt) (Fig. 2A). Three contigs were derived from the variants of known two fungal viruses: LeV-HKB (contig no. 74, 11340 nt) and LePV1 (a betapartitivirus, contig nos. 19 and 266, 2361 nt and 2220 nt, respectively). Other virus-like contigs appear to be sequences from a putative (–)ssRNA virus related to phenui-like viruses (contig nos. 296 and 1574, 7074 nt and 2773 nt, respectively), the previously unreported fungal ssRNA virus (contig nos. 315 and 10, related to accession no. AB647256), and four novel fungal (+)ssRNA viruses related to hypo-, fusari-, tymo-like and mitoviruses (Fig. 3A and LY, MF, and HK unpublished results).

To verify the presence of known fungal viruses (LeV-HKB and LePV1) and two novel (–)ssRNA virus-related RNAs in the shiitake sample, we performed RT-PCR using the specific primer sets for each of the fungal virus-like sequences. Using seven sets of primers (Table S1), we successfully amplified virus targets in the RNA samples extracted from the HG3 mycelia; but were unable to amplify any targets in the HG3 genomic DNA sample (Fig. 1D). After direct sequencing, the amplified cDNA fragments revealed identical sequences to the corresponding virus-like sequences obtained via deep RNA sequencing (data not shown). The remaining seven virus-like sequences (contig nos. 315, 10, and others) originating from novel or unpublished fungal (+)ssRNA viruses will be reported elsewhere.

Deep sequencing technologies can be utilized for the analysis of the RNA virome, uncovering a mixed-infection within single fungal strains of ascomycete (*Fusarium poae*) and basidiomycete (*Rhizoctonia solani*, *Sclerotium rolfsii* and *Agaricus bisporus*) (Bartholomäus et al., 2016; Deakin et al., 2017; Osaki et al., 2016; Zhu et al., 2018). Our deep sequencing analysis also successfully detected a mixed infection of diverse fungal RNA viruses, consisting of at least nine fungal viruses including two novel (–)ssRNA viruses (see details below, and LY, MF, and HK

unpublished results) in a single shiitake fungal strain (HG3). Because the shitake HG3 strain is co-infected with multiple fungal viruses, it is difficult to assess the phenotypic effects of each virus on the host fungus. For stable mushroom production, further studies using virus-cured and reintroduced strains are necessary to examine the effect of these fungal viruses on the host, particularly on fruiting body formation.

2.2. A novel non-segmented (−)ssRNA virus related to mymonaviruses

To verify the sequence of mymonavirus-like contig no. 585, obtained from next-generation sequencing (NGS) (Fig. 2A), overlapping RT-PCRs were performed and the amplified products were directly Sanger-sequenced from both directions (data not shown). The genome termini were determined by RNA ligase mediated (RLM) amplification of cDNA ends (RACE) (Fig. S1). The complete genome sequence of the mymona-like virus was 11,563 nt in length (Fig. 2B) and was deposited in the DNA Data Bank of Japan (DDBJ) (accession no. LC466007). This virus is the first mymonavirus known to infect basidiomycetes and has a significantly larger genome (11.6 kb) than other known mymonaviruses and mymonavirus-like agents (approximately 7.9–10 kb) (Liu et al., 2014; Marzano and Domier, 2016; Marzano et al., 2016; Wang et al., 2018b). We have tentatively designated the viral isolate as “Lentinula edodes negative-strand RNA virus 1 (LeNSRV1)”. The morphological characteristics of LeNSRV1 are still unknown, but two known mymonoviruses, Sclerotinia sclerotiorum negative-stranded RNA virus 1 (SsNSRV1) and Fusarium graminearum negative-stranded RNA virus 1 (FgNSRV-1), are thought to have filamentous virion and helical rod-like nucleocapsids, respectively (Liu et al., 2014; Wang et al., 2018b). The GC content of the LeNSRV1 RNA is 50.8%, slightly higher than that of other mymonaviruses (38.8–48.5%). The genome termini do not show obvious complementarity: only three terminal nucleotides share complementary, 3′-GAC…GUC-5′ (Fig. 2C). The viral genome (viral complimentary RNA strand, vcRNA) is predicted to have seven non-overlapping open reading frames (ORFs) (> 300 nt) (Fig. 2B). A semi-conserved AU-rich sequences is present in the putative untranslated sequences between ORFs in the LeNSRV1 genome (viral RNA strand, vRNA) (3′-AAAAUG/CUUUUUUUG-5′: type A for ORF1/2 and 3′-AAAAUUGUUUUUUUG-5′: type B for ORF4/5/6) (Fig. 2B and 2D). These semi-conserved sequences are most likely the

gene-junction sequences that commonly exist in the members of the order *Mononegaviridae* and are important for the transcription termination/polyadenylation and transcription initiations (Conzelmann, 1998). The 3' RACE analysis revealed that the 3'-terminal sequences of LeNSRV1 mRNAs were: ...UUUUAGAAAAAAA(A)n-3′ for ORF2 (N) protein and ...UUUUGAAAAAAA(A)n-3′ for ORF7 (L) protein (data not shown). Thus, the G residue following A/U-rich tracks (Fig. 2D, arrow), which is commonly found in the gene-junction of other mononegaviruses, such as rhabdoviruses (Kondo et al., 2014), might be important for the efficient transcription termination of the upstream gene, as demonstrated by previously (Barr et al., 1997; Whelan et al., 2000). The putative gene-junction sequence, in particular the type B sequence of LeNSRV1, is similar, but not identical, to those of mymona- and mymona-like viruses (Liu et al., 2014; Marzano et al., 2016; Wang et al., 2018b) (Fig. 2E), suggesting that the transcriptional regulation of mymonaviral genomes might also be well conserved.

The largest LeNSRV1 ORF (ORF7) encodes a large protein L (1969 aa, 221.8 kDa) with two typical domains, RdRp (accession no. cl15638, 6e-128) and mRNA capping region V (cl16796, 1e-08), and a conserved “GDNQ” tetra-peptide sequence in the RdRp core motif C, commonly found in mononegaviruses, including mymonaviruses. Among the seven LeNSRV1-encoded proteins, ORF2 and L proteins show moderate and significant amino acid sequence similarities to the putative nucleocapsid (or nucleoprotein, N) and L proteins of Hubei rhabdo-like virus 4 (HbRLV4), a mymonavirus identified from arthropods (host species unknown) meta-transcriptomics (N = 27.7% and L = 29.9%, respectively) (Shi et al., 2016), and L protein of other mymona- and mymona-like viruses (L = ~29.3–38.4%, respectively) (Kondo et al., 2013a; Liu et al., 2014; Marzano and Domier, 2016; Marzano et al., 2016; Wang et al., 2018b) (Table 1 and Fig. S2A for pairwise comparisons of viral proteins). However, the remaining five ORF (ORFs 1, 3–6) proteins do not have any significant similarity with other known viral proteins. The gene order of mymonaviruses does not seem to follow the general pattern in those of the mononegaviral genome (3′-N-P-M-G-L-5′) (Easton and Pringle, 2011). Unlike other mononegaviruses, except for orthopneumoviruseses, the genomes of LeNSRV1 and other characterized mymonaviruses contain a gene (ORF1 gene) upstream of the putative N (ORF2) gene (Liu et al., 2014; Marzano and Domier, 2016; Marzano et al., 2016; Wang et al., 2018b) (Fig. 2B), and the ORF6 of

LeNSRV1, whose position corresponds to that of glycoprotein G for mononegavirus, appeared to lack common structural features of the G protein (data not shown). In addition, whereas most known mymonaviruses have an additional small gene downstream of the L gene, it is absent in the genomes of LeNSRV1, HbRLV4 and other mononegaviruses (Fig. 2B). Thus, it is suggested that the acquisition of two small genes located at the 3′- (ORF1 gene) and 5′- terminal (a small ORF following the L gene) regions of the viruses may have occurred in ancestral mymonaviruses before and after the divergence of a group of LeNSRV1 and HbRLV4 (see below for the grouping).

In the maximum likelihood (ML) phylogenetic analysis using L proteins, the known mymonaviruses that infect ascomycete fungi (*Sclerotinia sclerotiorum*, *Fusarium graminearum* and *Botrytis cinerea*) and those associated with soybean plant leaves (except for soybean leaf-associated negative-stranded RNA virus 4 [SLaNSRV4, accession no. ALM6222]), and mymonavirus-like fungal TSA sequences (*Sclerotinia homoeocarpa*) formed two distinct sister clades (clades I and II) within the *Mymonaviridae* family (Fig. 3A and Table 1). In contrast, LeNSRV1, HbRLV4 and Kiln Barn virus—a mymona-like virus that infect the fruit fly (*Drosophila suzukii*) (accession no. AWA82236, a 3.7 kb contig sequence)—were placed in a well-supported distinct clade III within the *Mymonaviridae* family (Medd et al., 2018; Shi et al., 2016) (Fig. 3A and Table 1). This clade also consists of two mymonavirus-like transcriptome shotgun assembly (TSA) sequences (accession nos. GFHZ01022276 and GFLP01469011, respectively) derived from hybrid cultivars of sugarcane (*Saccharum* sp.) plants, in addition to a putative endogenous virus element (EVE) derived from a dicot powdery mildew fungus (*Golovinomyces cichoracearum*, formerly *Erysiphe cichoracearum*) whole genome shotgun sequence (WGS, accession no. MCBQ01018032) (Wu et al., 2018) (Figs. 3A, S2 and Table 1). A close phylogenetic relationship among LeNSRV1, HbRLV4 and putative *G. cichoracearum* EVE (accession no. RKF63845 and RKF80079) is also shown via the neighbor-joining (NJ) analysis based on N-like sequences (Fig. 3B and Table 1). The putative EVE sequences related to myomonaviral L proteins have also been discovered in the genome of other powdery mildew fungi, *Erysiphe pisi* and *Golovinomyces orontii,* representing possible molecular fossil records of ancient mymonavirus infection in their genomes (Kondo et al., 2015; Kondo et al., 2013a) (Fig.

S3). These EVE-like sequences are related to each other and are closely related to the clade III mononegaviruses (Fig. 3 and data not shown), showing an interesting insight into the long-term mymonaviral evolution and fungal host-virus coevolution.

2.3. A putative segmented (−)ssRNA virus related to phenuiviruses

The two phenuivirus-like elements identified from the HG3 NGS data (contig nos. 296 and 1574, with similar average coverage of 3182 and 3078 reads, respectively) might be derived from a novel (−)ssRNA virus related to the previously reported bipartite- or tripartite phenui-like viruses that are associated with plants and ticks (Navarro et al., 2018a; Navarro et al., 2018b; Tokarz et al., 2018; Xin et al., 2017) (see details below). Therefore, we tentatively designated this potential (−)ssRNA virus as "Lentinula edodes negative-strand virus 2 (LeNSRV2)". The entire sequence of LeNSRV2 was confirmed using direct sequencing of overlapping RT–PCR amplification products (data not shown) and RLM-RACE analysis of their termini (Fig. S1). The complete sequences of LeNSRV2 RNAs, namely RNA1 (contig no. 296) and RNA2 (contig no. 1574), were 7082 nt and 2754 nt, respectively (DDBJ Accession nos. LC466008 and LC466009) (Fig. 4B). The GC content of the two virus RNA elements was 37.2% for RNA1 and 40.5% for RNA2, which are similar values to the above mentioned plant- and tick-associated phenui-like viruses (35.7–38.5% for RNA1 and 35.1–40.1% for RNA2 and/or RNA3 segments). However, their entire RNA sequences have no significant similarity to that of other known viral genomes (data not shown). RNA1 and RNA2 (vRNA strand, negative sense) shared the first 10 nucleotides at 3′ terminus (3′-ACACAAAGAC…) and the first nine nucleotide at 5′ terminus (…UCUUUGUGU-5′) (Fig. 4B and C). Moreover, the first 9 nucleotide sequences of 3′ and 5′ termini of each RNA strand are complementary to each other (Fig. 4D). Such complementarity is common among many segmented (−)ssRNA viruses (Ferron et al., 2017), in particular in plant- and tick-associated phenui-like viruses. For example, citrus concave gum-associated virus (CCGaV, bipartite genome, a member of the newly established floating genus *Coguvirus,* which naturally infects citrus and apple trees) (Navarro et al., 2018a; Rott et al., 2018) and Laurel Lake virus (LLV, tripartite genome, derived from a pool of adalt *Ixodes scapularis* ticks) (Tokarz et al., 2018) , respectively. Sequence similarities are also found in a known phenuivirus, severe fever with thrombocytopenia

syndrome virus (SFTSV, in the genus *Banyangvirus*) (Fig. 4C), suggesting the potential of these sequences to form viral dsRNA panhandle structures that may plays a role in viral RNA encapsidation and the circularization viral RNA genome during formation of phenuiviral ribonucleoprotein (RNP) complex (Ferron et al., 2017; Hornak et al., 2016).

LeNSRV2 RNA1 (vcRNA strand) potentially codes for the large protein L (ORF1 protein: 2309 aa, 267.3 kDa), containing a Bunya_RdRp super family protein domain (accession no. cl20265, E-value = 2e-39) and the conserved "SDD" tri-peptide sequence in the RdRp catalytic motif C that are commonly found in the L protein of most segmented (−)ssRNA viruses. In addition, alignment of the N-terminal regions L protein of LeNSRV2 and those of related phenui-like viruses, uncovered the presence of a putative endonuclease domain with the key residue of cation dependent nucleases (the His+ endonucleases with the PD and the D/ExK motifs) (Holm et al., 2018; Sun et al., 2018) (Fig. S4). The L proteins endonuclease activity of phenuiviruses and most of other segmented (−)ssRNA viruses is likely to be essential for a unique mechanism known as "cap-snatching", in which the viral polymerase cleaves host mRNA via the endonuclease activity and utilizes its capped fragment for viral transcription (Holm et al., 2018; Sun et al., 2018). A BlastP analysis revealed that LeNSRV2 L protein shows significant amino acid sequence similarity (29.3–32.2% identity) to that of CCGaV and putative plant coguviruses, citrus virus A (CiV-A, bipartite genome, infects citrus trees, in association with no specific symptoms), watermelon crinkle leaf-associated virus 1 and 2 (WCLaV-1 and WCLaV-2, tripartite genome) (Navarro et al., 2018a; Navarro et al., 2018b; Rott et al., 2018; Wright et al., 2018; Xin et al., 2017), a tick-associated phenui-like virus (LLV) (Tokarz et al., 2018), and a previously unreported phenui-like fungal virus named Entoleuca bunyavirus 1 (EBV1: Accession no. AVD68666), from the ascomycete fungus *Entoleuca* sp. (the family Xylariaceae) (Table 1 and Fig. S2B for pairwise comparisons of viral proteins). The L protein also shows moderate amino acid sequence similarities (23.2–24.8% identity) to that of SFTSV isolates (data not shown).

LeNSRV2 RNA2 contains two ORFs (ORF2a and ORF2b), which are translated in the opposite direction to each other (Fig. 4B). These ORFs are separated by a noncoding 451-nt intergenic region (IGR, AU content 68.7%) that potentially forms a long A/U rich stem-loop structure (Fig.

S5). A similar coding scheme, with an intergenic A/U rich stem-loop structure, was observed for the RNA2 segments of two coguviruses (CCGaV and CiV-A) and therefore an ambisense coding strategy for these segments was proposed; this ambisense nature is similar to phleboviruses (tri-segment viruses) and tenuiviruses (multi-segment viruses) in the family *Phenuiviridae* (Navarro et al., 2018a; Navarro et al., 2018b) (see Fig. 4B). Therefore, the LeNSRV2 genome structure appears to be more closely related to that of bipartite coguviruses (CCGaV and CiV-A) than that of tripartite coguviruses (WCLaV-1 and WCLaV-2) or the tick-associated phenui-like virus (LLV) (Fig. 4B). No conserved domain was found in the LeNSRV2 ORF 2a protein (318 aa, 35.2 kDa), whereas ORF 2b protein (423 aa, 47.7 kDa) contains a conserved domain of the nucleocapsid protein (N) of phleboviruses and tenuiviruses (Tenui_N super family; accession no. cl05345, E-value = 3e-13) (Fig. 4B). BlastP analyses indicated that the ORF2a protein has moderate amino acid sequence similarities (21.8–23.5% identity) to that of the putative cell-to-cell movement protein (MP) of some coguviruses and a hypothetical protein (p2) of LLV (Table 1). The alignment based on both sequence and secondary structure similarities showed that LeNSRV2 ORF 2a protein, MP-like proteins of related phenui-like viruses and MPs of plant ophioviruses, members of the 30K MP superfamily (Borniego et al., 2016; Hiraguri et al., 2013) appeared to share similar key features including predicted beta-strand domains and a highly conserved aspartate (D) residue (see Mushegian and Elena, 2015; Navarro et al., 2018a) (Fig. S6). The ORF2b protein also shows moderate similarity (25.7–30.5% identity) to the putative N proteins of coguviruses, LLV, and apple rubbery wood virus 1 and 2 (ARWV-1 and ARWV-2, trip-segment viruses, in the suggested genus “Rubodvirus”) (Rott et al., 2018; Wright et al., 2018) (Table 1). Although LeNSRV2 and two bipartite coguviruses (CCGaV and CiV-A) predictably have ambisense coding strategy, their tripartite relatives (WCLaV-1 and WCLaV-2) do not. Moreover, the RNA2 and 3 segments of the WCLaVs have long U-rich 3′-terminal sequences and lack 5′- and 3′-terminal ends complementarity (Xin et al., 2017). In the case of our and previous studies, the NGS read coverage for the IGR of the ambisense viral segments was significantly low (Shi et al., 2018) (see also Fig. 4A). Thus, as also suggested by Navarro et al. (Navarro et al., 2018b), it cannot exclude the possibility that RNA2 and 3 of WCLaVs may be two contig fragments derived from a single ambisense RNA segment.

Based on the results, LeNSRV2 is most likely the first example of a segmented fungal (–)ssRNA virus related to phenuiviruses with the ambisense coding strategy. However, we could not find any additional LeNSRV2 segment(s) encoding for a precursor of glycoproteins (Gn/Gc) that are commonly encoded by a particular segment (namely M segment) of phenuiviruses and the recently discovered leishbuviruses (members of the newly established family *Leishbuviridae,* in the order *Bunyavirales*), which infect invertebrates and protists (Grybchuk et al., 2018) (see Fig. 5A for their phylogenetic relationships). Generally, the G protein(s) forms the membrane spikes of (–)ssRNA viral virions and are thought to play a critical role in host cell entry (Hornak et al., 2016). Thus, LeNSRV2 and related phenui-like viruses (coguviruses, rubodviruses and LLV) (Navarro et al., 2018a; Navarro et al., 2018b; Rott et al., 2018; Tokarz et al., 2018; Wright et al., 2018; Xin et al., 2017), may lack the M segment and/or G proteins because they have non-vertebrate hosts and thus probably do not have extracellular modes of transmission via enveloped virions. It is generally accepted that the replication of the (–)ssRNA viruses requires not only L polymerase but also the N protein, which is an essential viral factor for the formation of the RNP complex and scaffold for the replication process (Sun et al., 2018). Therefore, fungal (−)ssRNA viruses that are related to segmented (−)ssRNA viruses in the orders *Bunyavirales* and *Aspiviridae* (see the Introduction section) might also have additional RNA segment(s) encoding for the N protein and probably other viral protein(s).

An ML phylogenetic tree was constructed using L protein sequences derived from: representative members of 10 genera in the family *Phenuiviridae* (Maes et al., 2018); coguviruses; rubodviruses; LLV; and selected phenui-like viruses recently reported found in invertebrates (Li et al., 2015; Shi et al., 2016; Tokarz et al., 2018) and in fungi (Marzano et al., 2016; Osaki et al., 2016); and their recently discovered relatives, including leishbuviruses from invertebrates and protists (trypanosomatids, relatives of the human parasite *Leishmania*) (Grybchuk et al., 2018). The resulting ML tree shows that LeNSRV2 forms a well-supported clade together with coguviruses (CCGaV, CiV-A, WCLaV-1 and WCLaV-2), LLV, and the possible fungal phenui-like virus (EBV1) (Fig. 5A). LeNSRV2 is also distantly related to “rubodviruses” (ARWV-1 and ARWV-2) and representative phenuiviruses (shown as a triangle in the ML tree), as well as with other phenui-like viruses that infect an ascomycete fungus (*S. sclerotiorum*) and some invertebrate

species (Fig. 5A). Similar topology was also observed for the NJ trees based on N (ORF2b/ORF3) and MP-like (ORF2a/ORF2) proteins (Fig. 5B), indicating that the RNA2-encoded proteins of LeNSRV2 are more closely related to their analogs of plant coguviruses and related-viruses (LLV and EBV1) than those of plant "rubodviruses". Our phylogenetic analyses suggested that LeNSRV2 and related phenui-like viruses including members of the floating genus *Coguvirus* belong to the family *Phenuiviridae.* However, it is safer to wait until more phenui-like viruses are discovered to establish a novel genus (or genera) accommodating for LeNSRV2 and other related viruses (EBV1 and LLV) or to assign these viruses to the genus *Coguvirus*.

It has been proposed that the vertebrate- and plant-infecting bunyaviruses (within the order *Bunyavirales*) had been originated from arthropod-infecting progenitors and diverged to include important arthropod-borne pathogens of humans, animals, and plants (Li et al., 2015; Marklewitz et al., 2015). A similar evolutionary scenario could be accounted for host transitions of phenui-like viruses between ticks and fungi, such as in the case of the viral combinations (I) LLV and LeNSRV2 or EBV1, (II) Ixodes scapularis associated virus 5 and Fusarium poae negative-stranded virus 2, and (III) Ixodes scapularis associated virus 6 and Rhizictonia solani negative-strand virus 4 (Tokarz et al., 2018) (Fig. 5A). The close association between viruses that infect ticks and fungi has also been observed for reoviruses (in the family *Reoviridae*, have multi-segment dsRNA genome), tick-borne vertebrate coltiviruses, and fungal mycoreoviruses (Hillman et al., 2004). Therefore, the cross-kingdom virus transmission between ticks and fungi might have occurred over the evolutionary time scales. Another interesting evolutionary insight into the phenui-like viruses is the relationships between the viruses that infect plants (coguviruses) and fungi (LeNSRV2). The RNA segment of coguviruses and "rubodviruses" (bi- and tripartite plant phenui-like viruses) encodes for the putative MP-like gene (Navarro et al., 2018a; Navarro et al., 2018b; Rott et al., 2018; Wright et al., 2018; Xin et al., 2017), which might have been acquired by ancestral phenuivirus(es) to adapt to the plant hosts during their evolution (Dasgupta et al., 2001). A related MP-like gene is also presented in the LeNSRV2 RNA2 segment (Figs. 4B and 5B). Even though its function in the host(s) is still unknown, it gives rise to an interesting question whether this fungal virus could infect plants as an alternative viral host. Cross-kingdom viral infections between fungi and plants or fungi and arthropods (a mushroom fly) have recently

been demonstrated in the artificial and natural conditions (Andika et al., 2017; Liu et al., 2016; Mascia et al., 2014; Mascia et al., 2019; Nerva et al., 2017). Thus, it could be speculated that fungal species have potential as an alternative reservoir for coguviruses in natural environment. The investigations to prove these notions would provide a novel insight on the cross-kingdom viral infection of (–)ssRNA viruses between fungi and plants and/or fungi and ticks.

3. Conclusion

We have identified two novel fungal (–)ssRNA viruses, LeNSRV1 and LeNSRV2, that were discovered from shiitake via deep sequencing. Our finding on LeNSRV1 provides the first examples of a mymonavirus infecting basidiomycetes and shows that it has the largest genome compared to currently known other members. The second virus, LeNSRV2, is likely the first example of an fungal (–)ssRNA virus with a potential segmented genome, and is closely related to the recently discovered plant and tick phenui-like viruses and has a putative ambisense transcription strategy. The close relation between LeNSRV2 and other phenui-like viruses raise the possibility of cross-kingdom virus transfer between fungi and plants or fungi and ticks in ancient times and probably also present time. These findings enhance our understanding of the diversity, evolution, and spread of fungal (–)ssRNA viruses.

4. Materials and methods

4.1. *Lentinula edodes* strains

Commercially available fruiting bodies of shiitake (containing four cultured strains derived from different location, see Fig. 1A) were subject to screening for infection with unreported mymona-like virus infection. A shiitake strain (HG3) obtained from a fruiting body sample was grown on a cellophane-membrane over potato dextrose agar (PDA; BD Difco Laboratories, Detroit, MI, USA) plates at 22–25°C for further studies. For fungal species verification, fungal genomic DNA was isolated using DNeasy® Blood and Tissue Kit (Qiagen, Hilden, Germany) following the manufacturer's instructions and used for a template of polymerase chain reaction (PCR) amplification of the intergenic spacer region (ITS) using a primer set, ITS1 (5′-TCCGTAGGTGAACCTGCGG-3′) and ITS4 (5′-TCCTCCGCTTATTGATATGC-3′) of ribosomal RNA (White et al., 1990) (results not shown).

4.2. RNA extraction and RT-PCR

Total RNA from mushroom's fruiting bodies and mycelia was extracted using conventional phenol/chloroform treatment or TaKaRa RNAiso Plus Reagent (TaKaRa Biotech. Co., Shiga, Japan) using the acid guanidine-phenol-chloroform (AGPC) method, following the manufacturer's instructions. DsRNA fractions from fruiting bodies were isolated using CC41 cellulose (Whatman, USA) with the method as described previously (Sun and Suzuki, 2008). The total RNA and dsRNA-enriched fractions were analyzed using electrophoretic mobility on 1% agarose gel in 1× TAE buffer and stained with ethidium bromide. For reverse transcription (RT)-PCR detection, the cDNA strands were synthesized using MMLV or SuperScript II reverse transcriptase (Thermo Fisher Scientific, Waltham, MA, USA) and used as templates for PCR amplification with QuickTaq HS Dye Mix or KOD FX Neo Taq polymerase (Toyobo, Osaka, Japan). PCR products were then sequenced using the Sanger sequencing method.

4.3. Next-generation sequencing and reads assembly

Total RNA sample (645 ng/μL, RIN = 8.9) from shiitake HG3 strain was depleted rRNA with Ribo-Zero kit (Illumina, San Diego, CA, USA) and subjected to cDNA library construction using the TruSeq RNA Sample Preparation kit v2 (Illumina). The cDNA library was then subjected to deep sequencing (100 bp pair-end reads) using the Illumina HiSeq. 4000 platform (Illumina). The library construction and deep sequencing were performed by Macrogen Inc (Tokyo, Japan). After deep sequencing (Raw data: total read base, 11,250,881,062 bp; total reads, 111,394,862; GC content, 46.3%), the adaptors were trimmed and then the sequence reads (111,394,862 reads) were *de novo* assembled into 7,630 contigs (916–21,873 nt in length, set for a minimum contig length of 900 nt) using CLC Genomics Workbench (version 11, CLC Bio-Qiagen, Aarhus, Denmark). The assembled contigs were subjected to local BLAST searches against the viral reference sequence (RefSeq) dataset of National Center for Biotechnology Information (NCBI).

4.4. Reconfirmation of and terminal sequence determination of viral RNA sequences

To verify the sequence of the entire viral genomes, RT-PCR was performed using the sets of overlapping primers, and the amplified products were directly sequenced from both directions. Sequences of the primers used in overlapping RT-PCR are available upon request. For the 5′ and 3′ termini of the viral RNAs, 3′-RLM-RACE (Lin et al., 2012) was performed using total RNA extracted from the HG3 mycelia. Briefly, a 5′-phosphorylated oligodeoxynucleotide (3RACE-

adaptor, Table S1) was ligated to each of the 3′ termini of RNAs using T4 RNA ligase (Takara). The ligates were used as templates for cDNA synthesis in the presence of an oligodeoxynucleotide primer, complementary to the 3′-half of the 3RACE-adaptor (3RACE-1st, Table S1). The resulting cDNA was then amplified via PCR using the primer set 3RACE-2nd (which is complementary to the 5′ half of 3RACE-adaptor, Table S1) and virus-specific primers. To determine the 3′ termini of viral transcripts (mRNA), the 3′-RACE was performed using the FirstChoice® RLM-RACE kit (Ambion, Thermo Fisher Scientific), following the manufacturer's instructions. All PCR products were directly sequenced using the Sanger sequencing method.

4.5. Database search and sequence analysis

Viral sequence data were analyzed using GENETYX-MAC (Genetyx Co., Tokyo, Japan) or Enzyme X v3.3.3 (nucleobytes.com/enzymex/index.html). Sequence similarities were calculated using the BLAST program available from NCBI (nucleotide collection, nr/nt; transcriptome shotgun assembly, TSA) (http://blast.ncbi.nlm.nih.gov/Blast.cgi). Pairwise sequence identity was calculated using the Sequence Demarcation Tool (SDT) version 1.2 with the MUSCLE alignment (Muhire et al., 2014). The conserved protein domains were searched using the NCBI conserved domain database (CDD) (https://blast.ncbi.nlm.nih.gov/Blast.cgi). RNA secondary structures (stem-loop RNA structures) were predicted using Mfold version 2.3 (Zuker, 2003) (http://mfold.rna.albany.edu/). For MP-like proteins, multiple alignments of protein sequences and structures were performed using PROMALS3D (http://prodata.swmed.edu/promals3d/promals3d.php) (Pei et al., 2008).

4.6. Phylogenetic analyses

For phylogenetic reconstruction, maximum-likelihood (ML) tree construction was carried out according to a method as described previously (Kondo et al., 2019; Kondo et al., 2017). Multiple amino acid alignments were obtained by using MAFFT (Multiple Alignment using Fast Fourier Transform) verson 7 (Katoh and Standley, 2013) and refined using Gblocks 0.91b (Talavera and Castresana, 2007) with the stringency levels lowered for all parameters. ML phylogenetic trees were then generated using PhyML 3.0 (Guindon et al., 2010) with automatic model selection by Smart Model Selection (SMS) (http://www.atgc-montpellier.fr/phyml-sms/). The neighbor joining (NJ) trees (Saitou and Nei, 1987) were constructed based on the amino acid alignments using MAFFT. The phylogenetic trees (mid-point rooted) were visualized and refined using FigTree version 1.3.1 software (http://tree.bio.ed.ac.uk/software/).

Acknowledgements

We would like to thank Sakae Hisano and Kazuyuki Maruyama for their helpful technical assistance. We also thank the handling editor and two anonymous reviewers for their valuable suggestions. This study was supported by the Grants-in-Aid for Scientific Research (C) and on Innovative Areas from the Japanese MEXT (KAKENHI 15K07312, 16H06436, 16H06429 and 16K21723) and the Ohara Foundation for Agriculture Research. During review of this manuscript, Velasco et al. reported a fungal (–)ssRNA virus with a putative segmented genome in an ascomycete fungus (*Entoleuca* sp) (Velasco et al., 2019).

Conflicts of interest

The authors declare that there are no conflicts of interest.

Ethical statement

This article does not contain any studies with human participants or animals performed by any of the authors.

References

Ahn, I.P., Lee, Y.H., 2001. A viral double-stranded RNA up regulates the fungal virulence of *Nectria radicicola*. Molecular Plant-Microbe Interactions 14, 496-507.

Amarasinghe, G.K., Ceballos, N.G., Banyard, A.C., Basler, C.F., Bavari, S., et al., 2018. Taxonomy of the order *Mononegavirales*: update 2018. Archives of Virology 163, 2283-2294.

Andika, I.B., Wei, S., Cao, C.M., Salaipeth, L., Kondo, H., Sun, L.Y., 2017. Phytopathogenic fungus hosts a plant virus: A naturally occurring cross-kingdom viral infection. Proceedings of the National Academy of Sciences of the United States of America 114, 12267-12272.

Bartholomäus, A., Wibberg, D., Winkler, A., Pühler, A., Schlüter, A., Varrelmann, M., 2016. Deep sequencing analysis reveals the mycoviral diversity of the virome of an avirulent isolate of *Rhizoctonia solani* AG-2-2 IV. PloS ONE 11, e0165965.

Barr, J.N., Whelan, S.P.J., Wertz, G.W., 1997. Role of the intergenic dinucleotide in vesicular stomatitis virus RNA transcription. Journal of Virology 71, 1794-1801.

Borniego, M.B., Karlin, D., Peña, E.J., Luna, G.R., García, M.L., 2016. Bioinformatic and mutational analysis of ophiovirus movement proteins, belonging to the 30K superfamily. Virology 498, 172-180.

Conzelmann, K.K., 1998. Nonsegmented negative-strand RNA viruses: Genetics and manipulation of viral genomes. Annual Review of Genetics 32, 123-162.

Dasgupta, R., Garcia, B.H., Goodman, R.M., 2001. Systemic spread of an RNA insect virus in plants expressing plant viral movement protein genes. Proceedings of the National Academy of Sciences of the United States of America 98, 4910-4915.

Deakin, G., Dobbs, E., Bennett, J.M., Jones, I.M., Grogan, H.M., Burton, K.S., 2017. Multiple viral infections in *Agaricus bisporus* - Characterisation of 18 unique RNA viruses and 8 ORFans identified by deep sequencing. Scientific Reports 7, 2469.

Donaire, L., Pagan, I., Ayllon, M.A., 2016. Characterization of Botrytis cinerea negative-stranded RNA virus 1, a new mycovirus related to plant viruses, and a reconstruction of host pattern evolution in negative-sense ssRNA viruses. Virology 499, 212-218.

Easton, A.J., Pringle, C.R., 2011. Order Mononegavirales, in: King, A.M.Q., Adams, M.J., Carstens, E.B., Lefkowitz, E.J. (Eds.), Virus taxonomy: ninth report of the international committee on taxonomy of viruses. Elsevier, New York, pp. 653–657.

Ferron, F., Weber, F., de la Torre, J.C., Reguera, J., 2017. Transcription and replication mechanisms of *Bunyaviridae* and *Arenaviridae* L proteins. Virus Research 234, 118-134.

García, M.L., Dal Bó, E., da Graça, J.V., Gago-Zachert, S., Hammond, J., et al.,, 2017. ICTV virus taxonomy profile: *Ophioviridae*. Journal of General Virology 98, 1161-1162.

Ghabrial, S.A., Caston, J.R., Jiang, D.H., Nibert, M.L., Suzuki, N., 2015. 50-plus years of fungal viruses. Virology 479, 356-368.

Grybchuk, D., Akopyants, N.S., Kostygov, A.Y., Konovalovas, A., Lye, L.F., Dobson, D.E., Zangger, H., Fasel, N., Butenko, A., Frolov, A.O., Votypka, J., d'Avila-Levy, C.M., Kulich, P., Moravcova, J., Plevka, P., Rogozin, I.B., Serva, S., Lukes, J., Beverley, S.M., Yurchenko, V., 2018. Viral discovery and diversity in trypanosomatid protozoa with a focus on relatives of the human parasite *Leishmania.* Proceedings of the National Academy of Sciences of the United States of America 115, E506-E515.

Guindon, S., Dufayard, J.F., Lefort, V., Anisimova, M., Hordijk, W., Gascuel, O., 2010. New algorithms and methods to estimate maximum-likelihood phylogenies: assessing the performance of PhyML 3.0. Syst Biol 59, 307-321.

Guo, M.P., Bian, Y.B., Wang, J.J., Wang, G.Z., Ma, X.L., Xu, Z.Y., 2017. Biological and molecular characteristics of a novel partitivirus infecting the edible fungus *Lentinula edodes.* Plant Disease 101, 726-733.

Hao, F.M., Wu, M.D., Li, G.Q., 2018. Molecular characterization and geographic distribution of a mymonavirus in the population of *Botrytis cinerea.* Viruses-Basel 10, 432.

Hillman, B.I., Supyani, S., Kondo, H., Suzuki, N., 2004. A reovirus of the fungus *Cryphonectria parasitica* that is infectious as particles and related to the *Coltivirus* genus of animal pathogens. Journal of Virology 78, 892-898.

Hiraguri, A., Ueki, S., Kondo, H., Nomiyama, K., Shimizu, T., Ichiki-Uehara, T., Omura, T., Sasaki, N., Nyunoya, H., Sasaya, T., 2013. Identification of a movement protein of Mirafiori lettuce big-vein ophiovirus. Journal of General Virology 94, 1145-1150.

Holm, T., Kopicki, J.D., Busch, C., Olschewski, S., Rosenthal, M., Uetrecht, C., Gunther, S., Reindl, S., 2018. Biochemical and structural studies reveal differences and commonalities among cap-snatching endonucleases from segmented negative-strand RNA viruses. Journal of Biological Chemistry 293, 19686-19698.

Hornak, K.E., Lanchy, J.M., Lodmell, J.S., 2016. RNA encapsidation and packaging in the phleboviruses. Viruses-Basel 8, 194.

Katoh, K., Standley, D.M., 2013. MAFFT multiple sequence alignment software version 7: Improvements in performance and usability. Molecular Biology and Evolution 30, 772-780.

Kim, J.M., Yun, S.H., Park, S.M., Ko, H.G., Kim, D.H., 2013. Occurrence of dsRNA mycovirus (LeV-FMRI0339) in the edible mushroom *Lentinula edodes* and meiotic stability of LeV-FMRI0339 among monokaryotic progeny. Plant Pathology Journal 29, 460-464.

King, A.M.Q., Adams, M.J., Carstens, E.B., Lefkowitz, E.J., 2011. Virus taxonomy. Ninth report of the international committee on taxonomy of viruses. Elsevier Academic Press, London, San Diego

Komatsu, A., Kondo, H., Sato, M., Kurahashi, A., Nishibori, K., Suzuki, N., Fujimori, F., 2019. Isolation and characterization of a novel mycovirus infecting an edible mushroom, *Grifola frondosa*. Mycoscience, in press. https://doi.org/10.1016/j.myc.2019.01.005.

Kondo, H., Chiba, S., Maruyama, K., Andika, I.B., Suzuki, N., 2019. A novel insect-infecting virga/nege-like virus group and its pervasive endogenization into insect genomes. Virus Research 262, 37-47.

Kondo, H., Chiba, S., Suzuki, N., 2015. Detection and analysis of non-retroviral RNA virus-like elements in plant, fungal, and insect genomes. Methods in Molecular Biology 1236, 73-88.

Kondo, H., Chiba, S., Toyoda, K., Suzuki, N., 2013a. Evidence for negative-strand RNA virus infection in fungi. Virology 435, 201-209.

Kondo, H., Hirota, K., Maruyama, K., An'dika, I.B., Suzuki, N., 2017. A possible occurrence of genome reassortment among bipartite rhabdoviruses. Virology 508, 18-25.

Kondo, H., Kanematsu, S., Suzuki, N., 2013b. Viruses of the white root rot fungus, *Rosellinia necatrix*. Advances in Virus Research, Vol 86: Mycoviruses 86, 177-214.

Kondo, H., Maruyama, K., Chiba, S., Andika, I.B., Suzuki, N., 2014. Transcriptional mapping of the messenger and leader RNAs of orchid fleck virus, a bisegmented negative-strand RNA virus. Virology 452, 166-174.

Kormelink, R., Garcia, M.L., Goodin, M., Sasaya, T., Haenni, A.L., 2011. Negative-strand RNA viruses: The plant-infecting counterparts. Virus Research 162, 184-202.

Kotta-Loizou, I., Coutts, R.H.A., 2017. Mycoviruses in *Aspergilli*: A comprehensive review. Frontiers in Microbiology 8, 1699.

Kuhn, J.H., Wolf, Y.I., Krupovic, M., Zhang, Y.Z., Maes, P., Dolja, V.V., Koonin, E.V., 2019. Classify viruses — the gain is worth the pain. Nature 566, 318-320.

Lau, S.K., Lo, G.C., Chow, F.W., Fan, R.Y., Cai, J.J., Yuen, K.Y., Woo, P.C., 2018. Novel partitivirus enhances virulence of and causes aberrant gene expression in *Talaromyces marneffei.* mBio 9, e00947-00918.

Li, C.X., Shi, M., Tian, J.H., Lin, X.D., Kang, Y.J., Chen, L.J., Qin, X.C., Xu, J.G., Holmes, E.C., Zhang, Y.Z., 2015. Unprecedented genomic diversity of RNA viruses in arthropods reveals the ancestry of negative-sense RNA viruses. Elife 4, e05378.

Lin, Y.H., Chiba, S., Tani, A., Kondo, H., Sasaki, A., Kanematsu, S., Suzuki, N., 2012. A novel quadripartite dsRNA virus isolated from a phytopathogenic filamentous fungus, *Rosellinia necatrix*. Virology 426, 42-50.

Liu, L.J., Xie, J.T., Cheng, J.S., Fu, Y.P., Li, G.Q., Yi, X.H., Jiang, D.H., 2014. Fungal negative-stranded RNA virus that is related to bornaviruses and nyaviruses. Proceedings of the National Academy of Sciences of the United States of America 111, 12205-12210.

Liu, S., Xie, J.T., Cheng, J.S., Li, B., Chen, T., Fu, Y.P., Li, G.Q., Wang, M.Q., Jin, H.A., Wan, H., Jiang, D.H., 2016. Fungal DNA virus infects a mycophagous insect and utilizes it as a transmission vector. Proceedings of the National Academy of Sciences of the United States of America 113, 12803-12808.

Maes, P., Alkhovsky, S.V., Bao, Y.M., Beer, M., Birkhead, M., Briese, T., et al., 2018. Taxonomy of the family *Arenaviridae* and the order *Bunyavirales*: update 2018. Archives of Virology 163, 2295-2310.

Magae, Y., 2012. Molecular characterization of a novel mycovirus in the cultivated mushroom, *Lentinula edodes*. Virology Journal 9.

Magae, Y., Sunagawa, M., 2010. Characterization of a mycovirus associated with the brown discoloration of edible mushroom, *Flammulina velutipes*. Virology Journal 7, 342.

Marklewitz, M., Zirkel, F., Kurth, A., Drosten, C., Junglen, S., 2015. Evolutionary and phenotypic analysis of live virus isolates suggests arthropod origin of a pathogenic RNA virus family. Proceedings of the National Academy of Sciences of the United States of America 112, 7536-7541.

Marzano, S.Y.L., Domier, L.L., 2016. Novel mycoviruses discovered from metatranscriptomics survey of soybean phyllosphere phytobiomes. Virus Research 213, 332-342.

Marzano, S.Y.L., Nelson, B.D., Ajayi-Oyetunde, O., Bradley, C.A., Hughes, T.J., Hartman, G.L., Eastburn, D.M., Domier, L.L., 2016. Identification of diverse mycoviruses through metatranscriptomics characterization of the viromes of five major fungal plant pathogens. Journal of Virology 90, 6846-6863.

Mascia, T., Nigro, F., Abdallah, A., Ferrara, M., De Stradis, A., Faedda, R., Palukaitis, P., Gallitelli, D., 2014. Gene silencing and gene expression in phytopathogenic fungi using a plant virus vector. Proceedings of the National Academy of Sciences of the United States of America 111, 4291-4296.

Mascia, T., Vučurović, A., Minutillo, S.A., Nigro, F., Labarile, R., Savoia, M.A., Palukaitis, P., Gallitelli, D., 2019. Infection of *Colletotrichum acutatum* and *Phytophthora infestans* by taxonomically different plant viruses. European Journal of Plant Pathology, in press. https://doi.org/10.1007/s10658-018-01615-9.

Medd, N.C., Fellous, S., Waldron, F.M., Xuereb, A., Nakai, M., Cross, J.V., Obbard, D.J., 2018. The virome of *Drosophila suzukii*, an invasive pest of soft fruit. Virus Evolution 4, vey009.

Miles, P.G., Chang, S.T., 2004. Mushrooms: cultivation, nutritional value, medicinal effect, and environmental impact. 2nd ed. ed. CRC press, Boca Raton., p. 451.

Mu, F., Xie, J.T., Cheng, S.F., You, M.P., Barbetti, M.J., Jia, J.C., Wang, Q.Q., Chang, J.S., Fu, Y.P., Chen, T., Jiang, D.H., 2018. Virome characterization of a collection of *Sclerotinia sclerotiorum* from Australia. Frontiers in Microbiology 8, 2540.

Muhire, B.M., Varsani, A., Martin, D.P., 2014. SDT: A virus classification tool based on pairwise sequence alignment and identity calculation. Plos One 9, e108277.

Mushegian, A.R., Elena, S.F., 2015. Evolution of plant virus movement proteins from the 30K superfamily and of their homologs integrated in plant genomes. Virology 476, 304-315.

Navarro, B., Minutolo, M., De Stradis, A., Palmisano, F., Alioto, D., Di Serio, F., 2018a. The first phlebo-like virus infecting plants: a case study on the adaptation of negative-stranded RNA viruses to new hosts. Molecular Plant Pathology 19, 1075-1089.

Navarro, B., Zicca, S., Minutolo, M., Saponari, M., Alioto, D., Di Serio, F., 2018b. A negative-stranded RNA virus infecting citrus trees: the second member of a new genus within the order *Bunyavirales*. Frontiers in Microbiology 9, 2340.

Nerva, L., Varese, G.C., Falk, B.W., Turina, M., 2017. Mycoviruses of an endophytic fungus can replicate in plant cells: evolutionary implications. Scientific Reports 7, 1908.

Niu, Y.H., Yuan, Y.Z., Mao, J.L., Yang, Z., Cao, Q.W., Zhang, T.F., Wang, S.Q., Liu, D.L., 2018. Characterization of two novel mycoviruses from *Penicillium digitatum* and the related fungicide resistance analysis. Scientific Reports 8, 5513.

Nuss, D.L., 2005. Hypovirulence: Mycoviruses at the fungal-plant interface. Nature Reviews Microbiology 3, 632-642.

Osaki, H., Sasaki, A., Nomiyama, K., Tomioka, K., 2016. Multiple virus infection in a single strain of *Fusarium poae* shown by deep sequencing. Virus Genes 52, 835-847.

Ozkan, S., Coutts, R.H.A., 2015. Aspergillus fumigatus mycovirus causes mild hypervirulent effect on pathogenicity when tested on *Galleria mellonella*. Fungal Genetics and Biology 76, 20-26.

Pearson, M.N., Beever, R.E., Boine, B., Arthur, K., 2009. Mycoviruses of filamentous fungi and their relevance to plant pathology. Molecular Plant Pathology 10, 115-128.

Pei, J., Tang, M., Grishin, N.V., 2008. PROMALS3D web server for accurate multiple protein sequence and structure alignments. Nucleic Acids Research 36, 30-34.

Qiu, L.Y., Li, Y.P., Liu, Y.M., Gao, Y.G., Qi, Y.C., Shen, J.W., 2010. Particle and naked RNA mycoviruses in industrially cultivated mushroom *Pleurotus ostreatus* in China. Fungal Biology 114, 507-513.

Quesada-Moraga, E., Herrero, N., Zabalgogeazcoa, Í., 2014. Entomopathogenic and nematophagous fungal endophytes, in: VVerma, A.C., Gange, A.C. (Eds.), Advances in endophytic research. Springer, New Delhi, pp. 85-99.

Revill, P.A., Davidson, A.D., Wright, P.J., 1994. The nucleotide-sequence and genome organization of mushroom bacilliform virus - a single-stranded RNA virus of *Agaricus bisporus* (lange) imbach. Virology 202, 904-911.

Ro, H.S., Kang, E.J., Yu, J.S., Lee, T.S., Lee, C.W., Lee, H.S., 2007. Isolation and characterization of a novel mycovirus, PeSV, in *Pleurotus eryngii* and the development of a diagnostic system for it. Biotechnology Letters 29, 129-135.

Ro, H.S., Lee, N.J., Lee, C.W., Lee, H.S., 2006. Isolation of a novel mycovirus OMIV in Pleurotus ostreatus and its detection using a triple antibody sandwich-ELISA. Journal of Virological Methods 138, 24-29.

Rott, M.E., Kesanakurti, R., Berwarth, C., Rast, H., Boyes, I., Phelan, J., Jelkmann, W., 2018. Discovery of negative-sense RNA viruses in trees infected with apple rubbery wood disease by next-generation sequencing. Plant Disease 102, 1254-1263.

Ruigrok, R.W.H., Crepin, T., Kolakofsky, D., 2011. Nucleoproteins and nucleocapsids of negative-strand RNA viruses. Current Opinion in Microbiology 14, 504-510.

Rytter, J.L., Royse, D.J., Romaine, C.P., 1991. Incidence and diversity of double-stranded-RNA in *Lentinula edodes*. Mycologia 83, 506-510.

Sahin, E., Akata, I., 2018. Viruses infecting macrofungi. VirusDisease 29, 1-18.

Saitou, N., Nei, M., 1987. The neighbor-joining method - a new method for reconstructing phylogenetic trees. Molecular Biology and Evolution 4, 406-425.

Shi, M., Lin, X.D., Chen, X., Tian, J.H., Chen, L.J., Li, K., Wang, W., Eden, J.S., Shen, J.J., Liu, L., Holmes, E.C., Zhang, Y.Z., 2018. The evolutionary history of vertebrate RNA viruses. Nature 556, 197-202.

Shi, M., Lin, X.D., Tian, J.H., Chen, L.J., Chen, X., Li, C.X., Qin, X.C., Li, J., Cao, J.P., Eden, J.S., Buchmann, J., Wang, W., Xu, J., Holmes, E.C., Zhang, Y.Z., 2016. Redefining the invertebrate RNA virosphere. Nature 7634, 539-543.

Sun, L.Y., Suzuki, N., 2008. Intragenic rearrangements of a mycoreovirus induced by the multifunctional protein p29 encoded by the prototypic hypovirus CHV1-EP713. RNA 14, 2557-2571.

Sun, Y.P., Li, J., Gao, G.F., Tien, P., Liu, W.J., 2018. Bunyavirales ribonucleoproteins: the viral replication and transcription machinery. Critical Reviews in Microbiology 44, 522-540.

Talavera, G., Castresana, J., 2007. Improvement of phylogenies after removing divergent and ambiguously aligned blocks from protein sequence alignments. Systematic Biology 56, 564-577.

Tokarz, R., Sameroff, S., Tagliafierro, T., Jain, K., Williams, S.H., Cucura, D.M., Rochlin, I., Monzon, J., Carpi, G., Tufts, D., Diuk-Wasser, M., Brinkerhoff, J., Lipkin, W.I., 2018. Identification of novel viruses in *Amblyomma americanum*, *Dermacentor variabilis*, and *Ixodes scapularis* ticks. mSphere 3, e00614-17.

Ushiyama, R., 1979. Fungal viruses in edible fungi., Fungal Viruses. Springer, Berlin, Heidelberg., pp. p 25-33.

Velasco, L., Arjona-Girona, I., Cretazzo, E., López-Herrera, C., 2019. Viromes in Xylariaceae fungi infecting avocado in Spain. Virology 532, 11-21. https://doi.org/10.1016/j.virol.2019.03.021.

Walker, P.J., Blasdell, K.R., Calisher, C.H., Dietzgen, R.G., Kondo, H., et al., 2018. ICTV virus taxonomy profile: *Rhabdoviridae*. Journal of General Virology 99, 447-448.

Wang, J.J., Guo, M.P., Sun, Y.J., Bian, Y.B., Zhou, Y., Xu, Z.Y., 2018a. Genetic variation and phylogenetic analyses reveal transmission clues of Lentinula edodes partitivirus 1 (LePV1) from the Chinese *L. edodes* core collection. Virus Research 255, 127-132.

Wang, L., He, H., Wang, S.C., Chen, X.G., Qiu, D.W., Kondo, H., Guo, L.H., 2018b. Evidence for a novel negative-stranded RNA mycovirus isolated from the plant pathogenic fungus *Fusarium graminearum*. Virology 518, 232-240.

Whelan, S.P.J., Barr, J.N., Wertz, G.W., 2000. Identification of a minimal size requirement for termination of vesicular stomatitis virus mRNA: Implications for the mechanism of transcription. Journal of Virology 74, 8268-8276.

White, T.J., Bruns, T.S., Lee S, T., J., 1990. Amplification and direct sequencing of fungal ribosomal RNA genes for phylogenetics, in: Innis, M.A., Gelfand, D.H., Sninsky, J.J., White, T.J. (Eds.), PCR Protocols: A Guide to Methods and Applications. Academic Press Inc, San Diego, CA, USA, pp. 315–322.

Wolf, Y.I., Kazlauskas, D., Iranzo, J., Lucia-Sanz, A., Kuhn, J.H., Krupovic, M., Dolja, V.V., Koonin, E.V., 2018. Origins and evolution of the global RNA virome. mBio 9, e02329-18.

Won, H.K., Park, S.J., Kim, D.K., Shin, M.J., Kim, N., Lee, S.H., Kwon, Y.C., Ko, H.K., Ro, H.S., Lee, H.S., 2013. Isolation and characterization of a mycovirus in *Lentinula edodes*. Journal of Microbiology 51, 118-122.

Wright, A.A., Szostek, S.A., Beaver-Kanuya, E., Harper, S.J., 2018. Diversity of three bunya-like viruses infecting apple. Archives of Virology 163, 3339-3343.

Wu, Y., Ma, X.F., Pan, Z.Y., Kale, S.D., Song, Y., King, H., Zhang, Q., Presley, C., Deng, X.X., Wei, C.I., Xiao, S.Y., 2018. Comparative genome analyses reveal sequence features reflecting distinct modes of host-adaptation between dicot and monocot powdery mildew. BMC Genomics 19, 705.

Xie, J.T., Jiang, D.H., 2014. New insights into mycoviruses and exploration for the biological control of crop fungal diseases. Annual Review of Phytopathology 52, 45-68.

Xin, M., Cao, M.J., Liu, W.W., Ren, Y.D., Zhou, X.P., Wang, X.F., 2017. Two negative-strand RNA viruses identified in watermelon represent a novel clade in the order *Bunyavirales*. Frontiers in Microbiology 8, 1514.

Yu, X., Li, B., Fu, Y.P., Jiang, D.H., Ghabrial, S.A., Li, G.Q., Peng, Y.L., Xie, J.T., Cheng, J.S., Huang, J.B., Yi, X.H., 2010. A geminivirus-related DNA mycovirus that confers

hypovirulence to a plant pathogenic fungus. Proceedings of the National Academy of Sciences of the United States of America 107, 8387-8392.

Zhu, J.Z., Zhu, H.J., Gao, B.D., Zhou, Q., Zhong, J., 2018. Diverse, novel mycoviruses from the virome of a hypovirulent *Sclerotium rolfsii* strain. Frontiers in Plant Science 9, 1738.

Zuker, M., 2003. Mfold web server for nucleic acid folding and hybridization prediction. Nucleic Acids Research 31, 3406-3415.

Table 1. BlastP results for Lentinula edodes negative-strand virus 1 (LeNSRV1) and Lentinula edodes negative-strand virus 2 (LeNSRV2) proteins

Query/Virus or virus-like sequence name	protein	QC*	*E*-value	Identity	Accession
Query: LeNSRV1 L protein**					
Lentinula edodes helical virus		RdRp	23%	0.0	99.6%	AGH07920
Hubei rhabdo-like virus 4		RdRp	90%	0.0	29.9%	
	YP_009336595				
Golovinomyces cichoracearum EVE1***		RdRp	58%	0.0	35.1%	RKF58740
Kiln Barn virus		HP*	51%	0.0	38.4%	AWA82236
Sclerotinia sclerotiorum negative-stranded RNA virus 1	L	61%	2e-139	29.3%	YP_009094317	
Sclerotinia sclerotiorum negative-stranded RNA virus 3	RdRp	59%	4e-139	30.2%	YP_009129259	
Soybean leaf-associated negative-stranded RNA virus 4	RdRp	54%	1e-137	31.4%	ALM62229	
Query: LeNSRV1 ORF2 protein					
Golovinomyces cichoracearum EVE2		HP_GcM1	66%	3e-14	25.2%	RKF63845
Hubei rhabdo-like virus 4		HP2	63%	4e-13	27.7%	
	YP_009336594				
Golovinomyces cichoracearum EVE3		HP_GcM3	19%	1e-05	38.2%	RKF77081
Query: LeNSRV2 L protein (RNA1) **					
citrus concave gum-associated virus		RdRp	79%	0.0	32.2%	AXR98526
watermelon crinkle leaf-associated virus 1		RdRp	77%	0.0	31.8%	ASY01340
watermelon crinkle leaf-associated virus 2		RdRp	78%	0.0	31.7%	ASY01343
citrus virus A		RdRp	77%	0.0	31.8%	AYN78568
Laurel Lake virus		RdRp	87%	0.0	29.5%	ASU47549
Entoleuca bunyavirus 1		replicase	76%	0.0	29.3%	AVD68666
severe fever with thrombocytopenia virus		RNA pol.	73%	4e-101	24.7%	ATW62994
Query: LeNSRV2 MP-like protein (RNA2, 2a protein)					
citrus concave gum-associated virus		p46	53%	8e-17	23.5%	AXR98528
citrus virus A		MP*	58%	2e-15	23.1%	AYN78569
Laurel Lake virus		P2	47%	2e-12	28.4%	AUW34409
watermelon crinkle leaf-associated virus2	MP	55%	1e-06	21.8%	ASY0134	
Query: LeNSRV2 nucleocapsid-like protein (RNA2, 2b protein) **					
Laurel Lake virus		NP*	63%	1e-16	25.7%	ASU47550
citrus concave gum-associated virus.		NP	52%	1e-11	27.3%	AXR98527
apple rubbery wood virus 1		CP*	65%	4e-08	29.6%	AWC67524
Tacheng tick virus 2		NP	43%	2e-07	30.5%	AJG39316
apple rubbery wood virus 2		CP	56%	1e-05	27.1%	AWC67532
Kismayo virus		NP	46%	2e-05	26.0%	AIU95035
Changping tick virus 1		NP	47%	4e-05	27.4%	AJG39302

*: Query cover; HP: hypothetical protein; NP: nucleocapsid protein; CP: capsid protein; MP: putative movement protein.

**: selected top seven hits.

***: *Golovinomyces cichoracearum* WGS sequences, putative endogenous viral elements (EVEs).

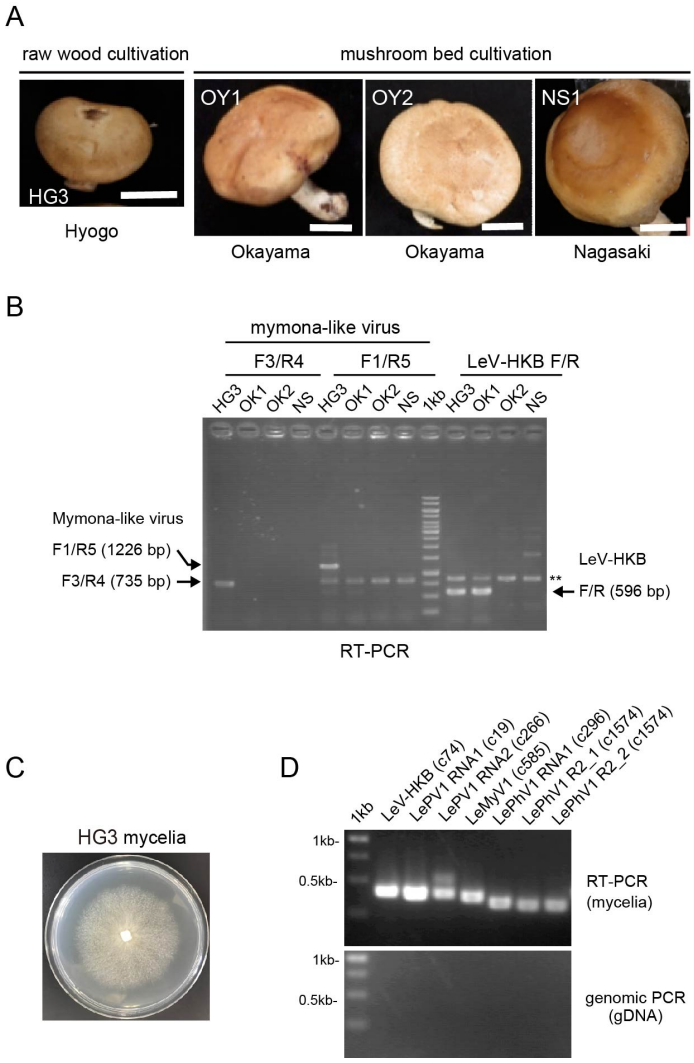

Fig. 1. The presence of fungal viruses in shiitake (*Lentinula edodes*) strains. **(A)** shiitake fruiting bodies that grow on hardwood logs (HG3 strain) in Hyogo and some other commercially available strains that are grown on artificial sawdust media (mushroom bed) in Okayama (OK1 and OK2, two different suppliers) and Nagasaki (NS) prefectures. **(B)** RT-PCR detection of a putative mymonavirus and LeV-HKB using total RNA preparations from shiitake fruiting bodies. **: asterisks show non-specific amplification products; 1kb: DNA size marker (GeneRuler 1 kb DNA ladder, Thermo Fisher Scientific., Inc., Waltham, MA, USA). **(C)** Colony morphology of shiitake strain HG3. The isolate was grown on PDA for three weeks and photographed. **(D)** RT-PCR and genomic PCR detection of the fungal virus-like sequences (see Table 1) in the total RNA or DNA samples derived from the HG3 strain. DNA was stained with ethidium bromide. Primer sets used for RT-PCR (B and D) are listed in Table S1. The quality of DNA used for genomic PCR was validated by amplification of ITS region using a primer set (ITS1 and ITS4) (data not shown).

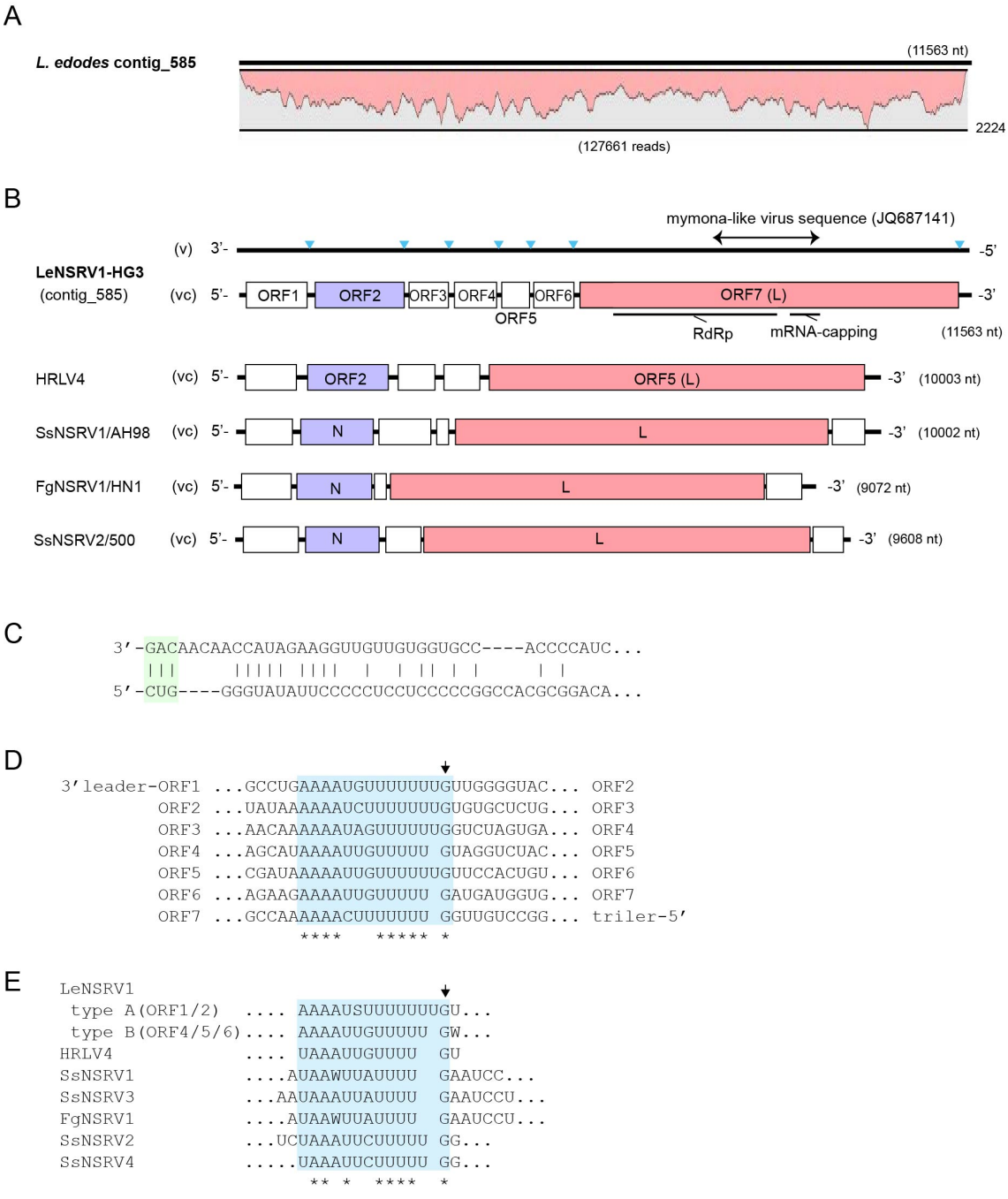

Fig. 2. Genome organization and phylogeny of a novel mononegavirus from the shiitake strain HG3. (**A**) Read depth coverage across the novel mononega virus-assembled contig (no. 585, 11568 nt) (**B**) Schematic representation of the genomic organization of Lentinula edodes negative-strand RNA virus 1-HG3 (LeNSRV1-HG3) and three related mymona- or mymona-like viruses, Hubei rhabdo-like virus 4 (HbRLV4, derived from an arthropod mix, accession number NC_032783), Sclerotinia sclerotiorum negative-stranded RNA virus 1 and 2 (SsNRV1 and 2,

KJ186782 and KP900931, respectively) and Fusarium graminearum negative-stranded RNA virus 1 (FgNSRV-1, MF276904). (v) and (vc) are indicate genomic and anti-genomic RNAs, respectively. The triangles in the genomic RNA and the boxes in the anti-genomic RNA show putative gene junctions and open reading frames (ORFs), respectively. The putative conserved domains for RNA-dependent RNA polymerase (RdRp) and mRNA capping are indicated below the ORF. Genome organizations of mymona- or mymona-like viruses are shown with the anti-genomic RNA strands. (**C**) Complementarity between the 3′- and 5′-terminal sequences of LeNSRV1 genomic RNA (3′–5′, negative). Vertical lines between the sequences indicate complementary nucleotides. (**D**) Comparison of putative gene-junctions between ORFs in the LeNSRV1 genome. Alignment of the putative junction sequences are shown in the 3′-to-5′ orientation. Conserved sequences are highlighted. **(E)** Consensus sequences of gene junction regions in mymonaviral genomes. The gene junction sequences compared here are derived from other mymona- or mymona-like viruses, whereas some junction sequences are not well conserved. Arrows indicate the conserved G residue following A/U-rich tracks, which is commonly found in the gene-junction of other mononegaviruses. W: A or U; S: C or G (the IUB code).

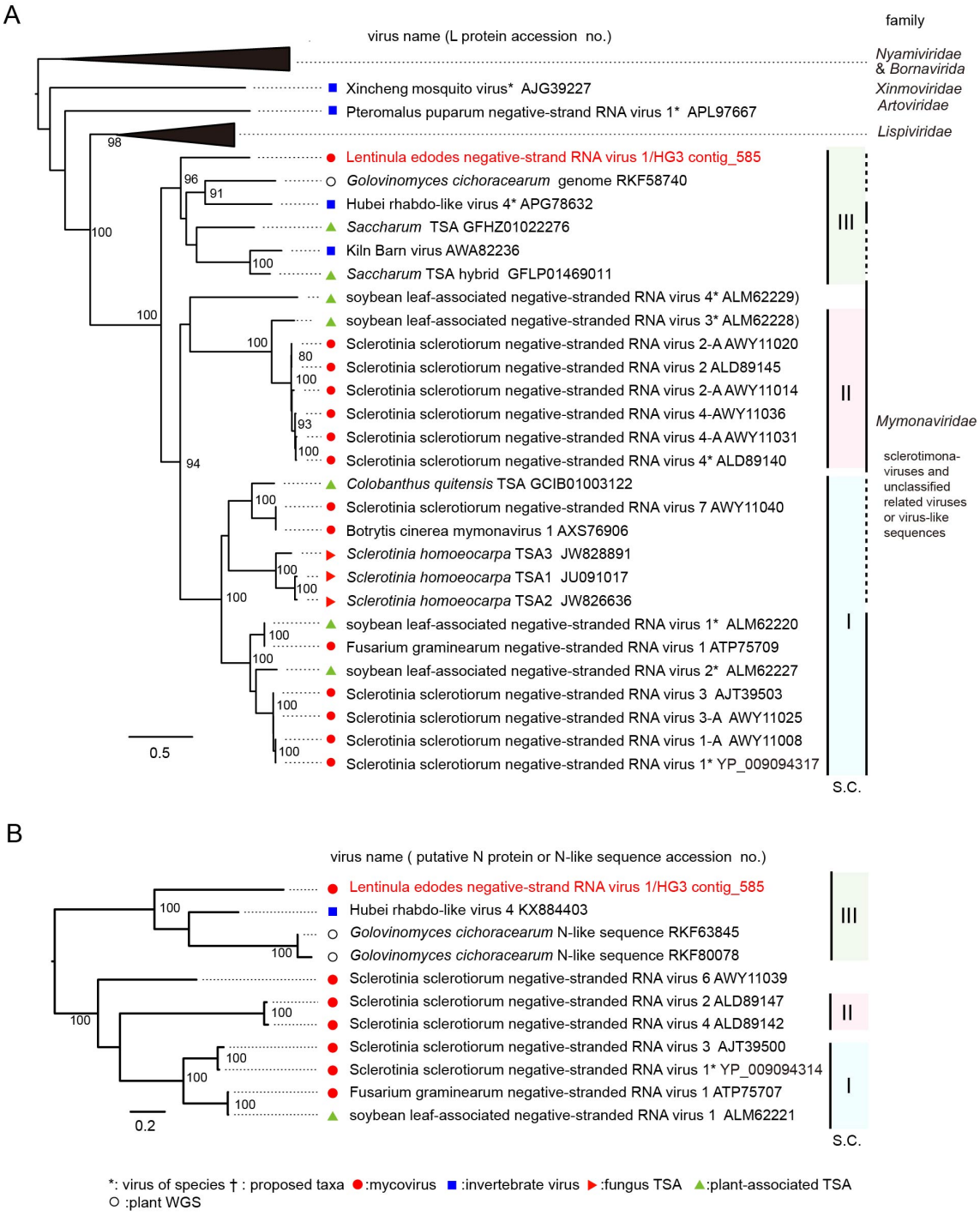

Fig. 3. Phylogenetic relationships of LeNSRV1 and related mymona- or mymona-like viruses from fungi and animals (mainly metatranscriptome of arthropod samples). **(A)** The maximum-likelihood (ML) tree was constructed using a multiple amino acid sequence alignment of entire L polymerases. The results of this multiple alignment together with that of subsequent analyses for other viral proteins, are available upon request. L proteins from unclassified mymona- or mymona-like viruses, mymonavirus-like transcriptome shotgun assemblies (TSAs), and a

putative endogenous virus element (EVE) derived from the powdery mildew fungus (*Golovinomyces cichoracearum*) are also included in this analysis. **(B)** The neighbor joining (NJ) tree was constructed using a multiple amino acid sequence alignment of nucleocapsid (N) or N-like proteins encodedby each ORF2 in the virus genomes. The putative *G. cichoracearum* EVEs are also included. Virus names are followed by GenBank accession numbers (see Table S2 for the virus names in the collapsed triangles). Three sister clades within the family *Mymonaviridae* are indicated (clades I–III). The scale bar represents amino acid distances. The numbers at the nodes are bootstrap values of > 90%.

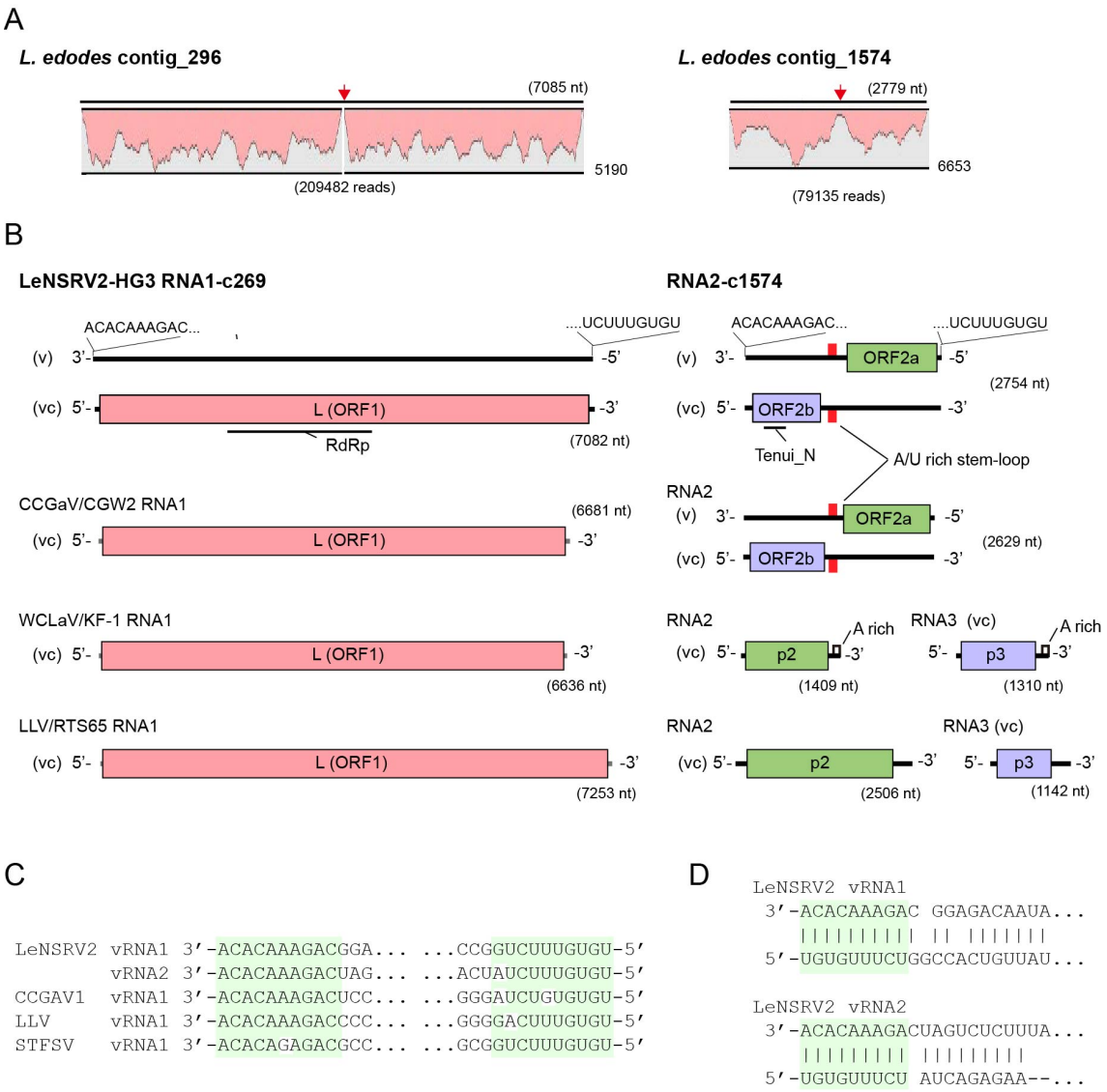

Fig. 4. Genome organization and phylogeny of a novel (–)ssRNA virus with a potential segmented genome from the shiitake strain HG3. (**A**) Read depth coverage across the novel (–)ssRNA-assembled contigs (nos. 296 and 1574, 17085 nt and 2779 nt, respectively). The arrows show a miss-assembly site in contig no. 296 (the actual genome sequence was verified by cDNA sequencing) and the region in the contig no. 1574 where the read coverage is significantly low, respectively. (**B**) Schematic representation of the putative genomic organization of Lentinula edodes negative-strand RNA virus 2-HG3 (LeNSRV2-HG3) and two plant phenui-like viruses, citrus concave gum-associated virus (CCGaV, accession numbers RNA1 and 2: KX960112 and KX960111, respectively) and watermelon crinkle leaf-associated virus 1 (WCLaV-1, RNA1–3: KY781184–6). Also a tick-associated phenui-like virus, Laurel Lake virus (LLV, RNA1–3: KX774630, MG256515 and KX774631). (v) and (vc) indicate genomic and anti-genomic RNAs, respectively. The putative RNA2 segment of LeNSRV2 and CCGaV shows potential ambisense coding strategy. The putative conserved domains or sequences for RdRp and tenuiviral

nucleocapsid protein (Tenui_N) are indicated below the LeNSRV2 ORFs. Stem loops in the intergenic region of both RNA2 strands of LeNSRV2 and CCGaV (see also Fig. S4) and 3′-terminal long A-rich sequences (vc strand of WCLaV-1) are indicated by the small filled- and open-boxes, respectively. (**C**) Comparison of LeNSRV2 genomic RNA termini with those of CCGaV, LLV, and severe fever with thrombocytopenia syndrome virus (a banyangvirus, in the family *Phenuiviridae*). (**D**) Complementary structure between the 3′ and 5′ termini in the putative LeNSRV2 genome.

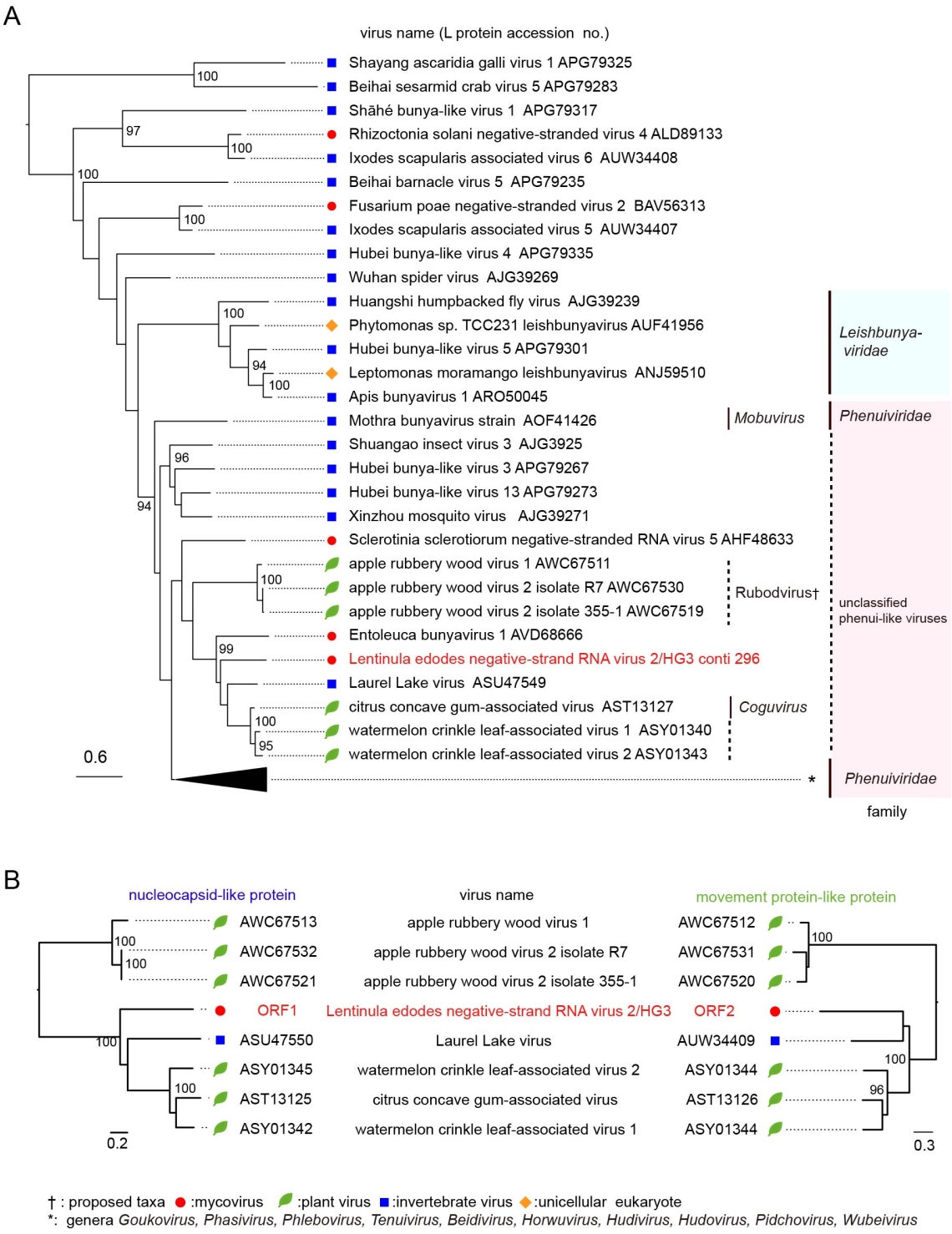

Fig. 5. Phylogenetic relationships of LeNSRV2 and related phenui- or phenui-like (–)ssRNA viruses from fungi, plants, and animals. **(A)** The ML tree was constructed by using a multiple amino acid sequence alignment of the entire sequence of L polymerases. L proteins from representative members of 10 genus in the family *Phenuiviridae*, coguviruses, rubodviruses, LLV and recent reported selected phenui-like viruses from invertebrates and fungi are included in this

analysis. Phenuivirus-related viruses (family *Leishbuviridae*) derived from the invertebrates and unicellular eukaryotes (*Leptomonas moramango* and *Phytomonas* sp. in the family *Trypanosomatidae*) are also included. **(B)** NJ phylogenetic trees were constructed using MAFFT version 7 based on the multiple amino acid sequence alignment of the potential nucleoproteins (NC) (left side tree) and putative movement protein (MP)-like or p2 (unknown faction) proteins (right side tree). Virus names are followed by GenBank accession numbers (see Table S2 for the virus names in the collapsed triangle). The scale bar represents amino acid distances. The numbers at the nodes are bootstrap values of > 90%.

Supplementary Material

Table S1. Primer list

Primer name	sequence (5' to 3')	usage	
Lentinula edodes mycovirus HKB (LeV-HKB)			
LeV-HKB F	GCTTCACGGAGAGTGAGTACACCCG	RT-PCR for ORF2	Fig. 1B
LeV-HKB R	CTAAATGGTCAGCCCTCTGTTTGCG	RT-PCR for ORF2	Fig. 1B
HG3_LeV-HKB-F	TGTTGTATAAGACAGGCGGTGTGGG	RT-PCR for ORF2	Fig. 1D
HG3_LeV-HKB-R	GGGTATATCTCAGCAAGCCTATGC	RT-PCR for ORF2	Fig. 1D
Lentinula edodes partitivirus 1 (LePV)			
HG3_LePVRd-F	AGCCTTTGACGATGTATCCGACTAC	RT-PCR for RNA1	Fig. 1D
HG3_LePVRd-R	GGGTTATGATTGCGAGAGGCATT	RT-PCR for RNA1	Fig. 1D
HG3_LePVCP-F	ACTACCCGTATGGTCTCCATACCGG	RT-PCR for RNA2	Fig. 1D
HG3_LePVCP-R	CAAATGGTGAAAAAGCATTCGCT	RT-PCR for RNA2	Fig. 1D
Lentinula edodes negative-strand RNA virus 1 (LeNSRV1)			
mymona like F1	AACCATGACCTGAAGCCAGAGGAGTG	RT-PCR for ORF7	Fig. 1B
mymona like F3	GCTCACTGGACAAGGTGATAACGTTA	RT-PCR for ORF7	Fig. 1B
mymona like R4	CCCACTCTGTCAGACGGGGACACAGGC	RT-PCR for ORF7	Fig. 1B
mymona like R5	AGACTGAGTTTCCTAAGAGCTGAGGC	RT-PCR for ORF7	Fig. 1B
HG3_c585_8111F	CGAGACATCCTCGCGGCTGTAGAGG	RT-PCR for ORF7	Fig. 1D
HG3_c585_8487R	CCGAGGTTACCAGCTCCGATTGTC	RT-PCR for ORF7	Fig. 1D
HG3_c585_Ra-F1	GGGGCGGATCAGCCGCTGGAAGCAC	3'-RLM-RACE for vRNA1	Fig. S3
HG3_c585_Ra-F2	GTTGAATCCCTCATTGAACACACGC	3'-RLM-RACE for vRNA1	Fig. S3
HG3_c585_Fa-F1	CGGAGTGTCAGTCTCAACCTCCGTC	3'-RLM-RACE for vcRNA1	Fig. S3
HG3_c585_Fa-F2	CAGAGCAGACTGTCGAGCTGCGACG	3'-RLM-RACE for vcRNA1	Fig. S3
Lentinula edodes negative-strand RNA virus 2 (LeNSRV2)			
HG3_c296_3396F	AAGTATGGGGTAGTGATGATAGTGG	RT-PCR for RNA1 ORF1	Fig. 1D
HG3_c296_3723R	GAGGCTCCACCTTCCAATGTCTGAG	RT-PCR for RNA1 ORF1	Fig. 1D
HG3_c296_Ra-R1	GAGTCAATGGGCAGTTACTGAGTAC	3'-RLM-RACE for vRNA1	Fig. S3
HG3_c296_Ra-R2	GATAAGGGGACATCTGTCTCGTCAC	3'-RLM-RACE for vRNA1	Fig. S3
HG3_c296_Ra-F1	TGCAGCACTAACCCAGTTCTGTAGG	3'-RLM-RACE for vcRNA1	Fig. S3
HG3_c296_Ra-F 2	TCTTATCTGGATTCCTTACCTTCTC	3'-RLM-RACE for vcRNA1	Fig. S3
HG3_c1574_842F	GGCAAGCAGCCCTCTTCAATCTCGG	RT-PCR for RNA2 ORF2b, set 1	Fig. 1D
HG3_c1574_1159R	CTCGGCTGACCAGGCATGGATG	RT-PCR for RNA2 ORF2b, set 1	Fig. 1D
HG3_c1574_2363F	GAAGTGCAAGTCTTTCTTCTGGAGA	RT-PCR for RNA2 ORF2a, set 2	Fig. 1D
HG3_c1574_2682R	AAGCCGTTGAGAGAGAAGAAGCTCC	RT-PCR for RNA2 ORF2a, set 2	Fig. 1D
HG3_c1574_Ra-R1	CCTAGGCAGTGTTACAGCCAACCTC	3'-RLM-RACE for vRNA1	Fig. S3
HG3_c1574_Ra-R2	TACTGAGGCCATCCTATGTTTCCTGC	3'-RLM-RACE for vRNA1	Fig. S3
HG3_c1574_Ra-F1	TTGACCTTACCAGGCTCTCTTCCAC	3'-RLM-RACE for vcRNA2	Fig. S3
HG3_c1574_Ra-F2	CAAATCATAACTCCTAACAGATGCC	3'-RLM-RACE for vcRNA2	Fig. S3
3'RNA ligase mediated amplification of cDNA ends			
3RACE-adaptor	(PO_4)-CAATACCTTCTGACCATGCAGTGACAGTCAGCATG		
3RACE-1st	CATGCTGACTGTCACTGCAT		
3RACE-2nd	TGCATGGTCAGAAGGTATTG		

Table S2. List of virus and accession numbers of the L-polymerase compared in Figs 3 and 5 (shown as rectangles).

Taxa/ Genus	Virus name	Genbank/ Ref seq. accession	
Fig. 3 rectangles			
Order *Mononegavirales*			
Family *Nyamiviridae*			
Nyavirus	Nyamanini virus	YP_002905337	Fig. 3A
Socyvirus	soybean cyst nematode virus 1	AEF56729	Fig. 3A
Berhavirus	Beihai rhabdo-like virus 3	KX884408	Fig. 3A
Orivirus	Orinoco virus	KX257488	Fig. 3A
Crustavirus	Wenzhou crab virus 1	AJG39154	Fig. 3A
Tapwovirus	Wenzhou tapeworm virus 1	KX884436	Fig. 3A
Family *Bornavirida*			
Bornavirus	Borna disease virus 1	NP_042024	Fig. 3A
Family *Lispiviridae*			
Arlivirus	Lishi spider virus 2	AJG39111	Fig. 3A
	Sanxia water strider virus 4	AJG39115	Fig. 3A
	Tacheng tick virus 6	AJG39142	Fig. 3A
Fig. 5 rectangle			
Order *Bunyavirales*			
Family *Phenuiviridae*			
Goukovirus	Gouleako virus	AEJ38175	Fig. 5A
Phasivirus	Badu virus	AMA19446	Fig. 5A
Phlebovirus	Rift Valley fever virus	YP_003848704	Fig. 5A
Tenuivirus	rice stripe virus	NP_620522	Fig. 5A
Beidivirus	Hubei diptera virus 3	APG79285	Fig. 5A
Horwuvirus	Wuhan horsefly virus	AJG39260	Fig. 5A
Hudivirus	Hubei diptera virus 4	APG79298	Fig. 5A
Hudovirus	Hubei lepidoptera virus 1	APG79261	Fig. 5A
Pidchovirus	Pidgey virus	KX852391	Fig. 5A
Wubeivirus	Wuhan fly Virus 1	AJG39259	Fig. 5A

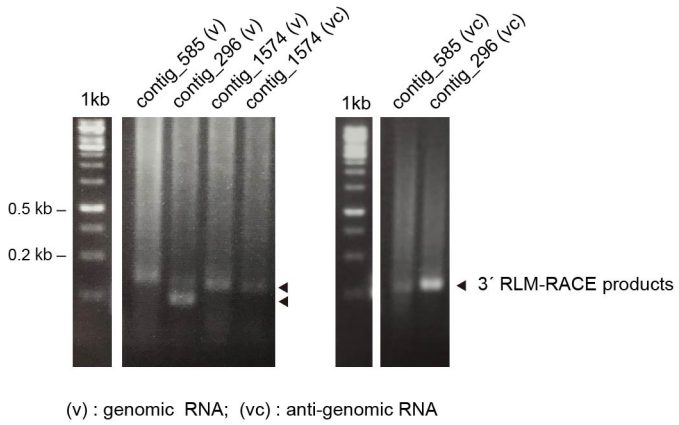

Fig. S1. The RLM-RACE (RNA ligase-mediated RACE) analyses of two novel fungal (–)ssRNA viruses from the shiitake strain HG3. Agarose gel electrophoresis of 3′ RLM-RACE products derived from Lentinula edodes negative-strand RNA virus 1 (LeNSRV1-HG3) and Lentinula edodes negative-strand RNA virus 2 (LeNSRV2-HG3) RNA segments was performed. The 3′ terminal sequences of each viral RNA segments were determined by direct sequencing of the 3′ RLM-RACE amplification products.

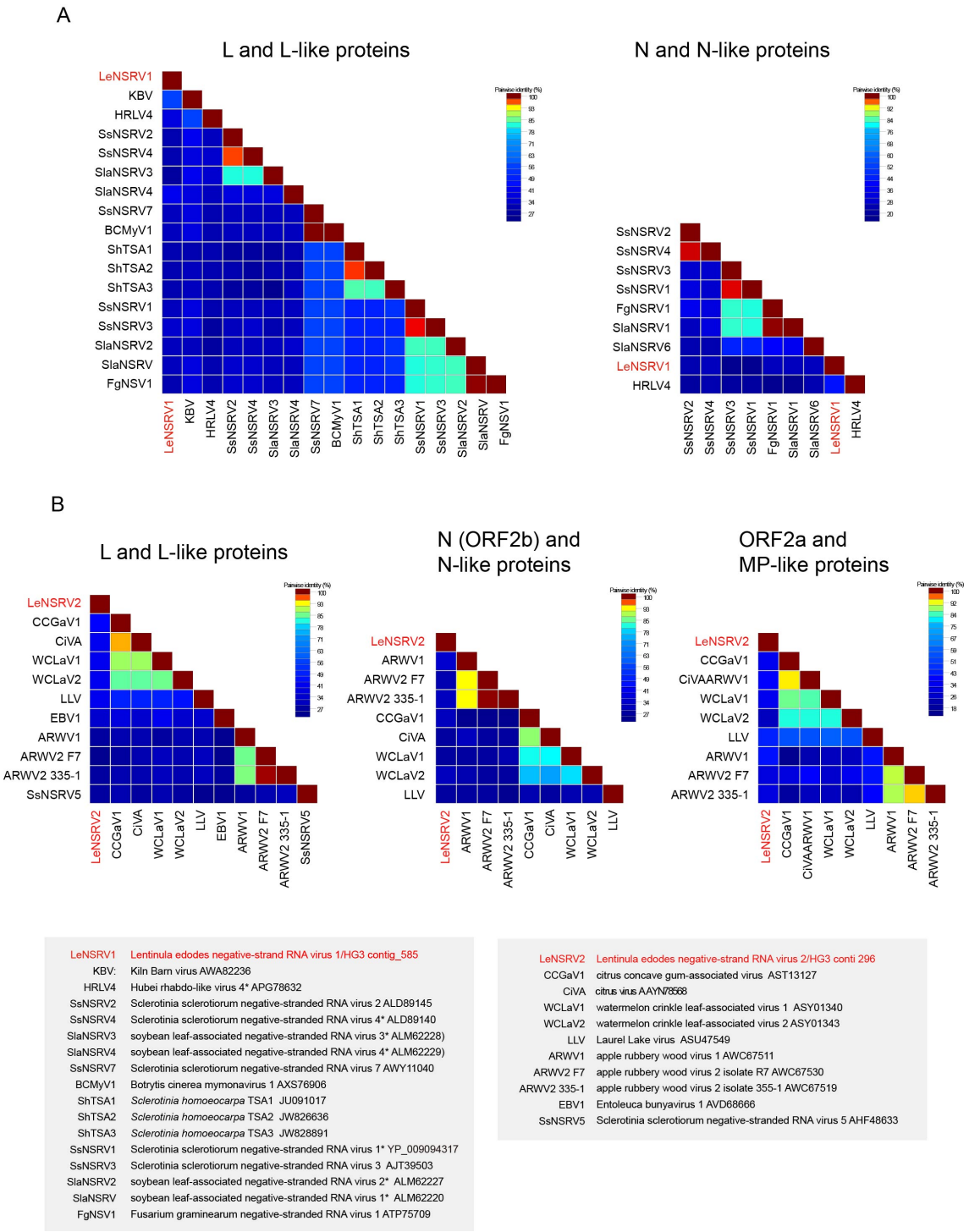

Fig. S2. Pairwise comparison of viral proteins encoded by LeNSRV1-HG3 and LeNSRV2-HG3. Each color represents the relative pairwise amino acid identities (%) between corresponding viral proteins, calculated using SDT version 1.2 (Muhire et al., 2014).

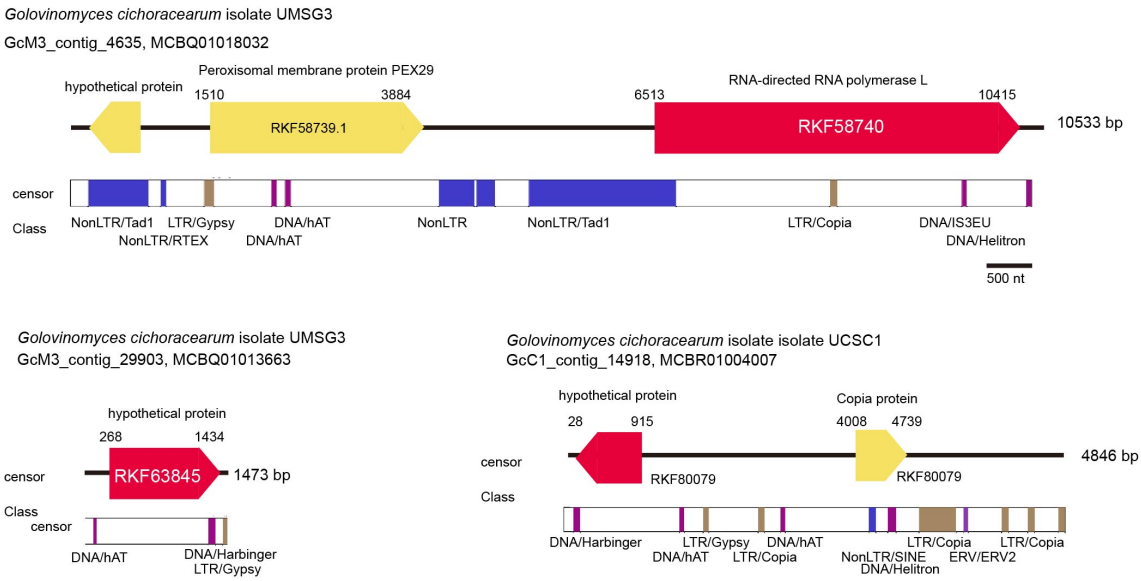

Fig. S3. Schematic representation of mymonavirus-like endogenous viral elements (EVEs) and their flanking regions. EpMLLSs found in the *Golovinomyces cichoracearum* genomic DNAs. Top row for each genomic sequence shows a diagrammatic representation of the potential coding regions of *G. cichoracearum* EVEs and flanking genes/ORFs, indicated as boxes with red and yellow color, respectively. Bottom row shows potential transposable element sequences predicted using Censor (https://www.girinst.org/censor/index.php).

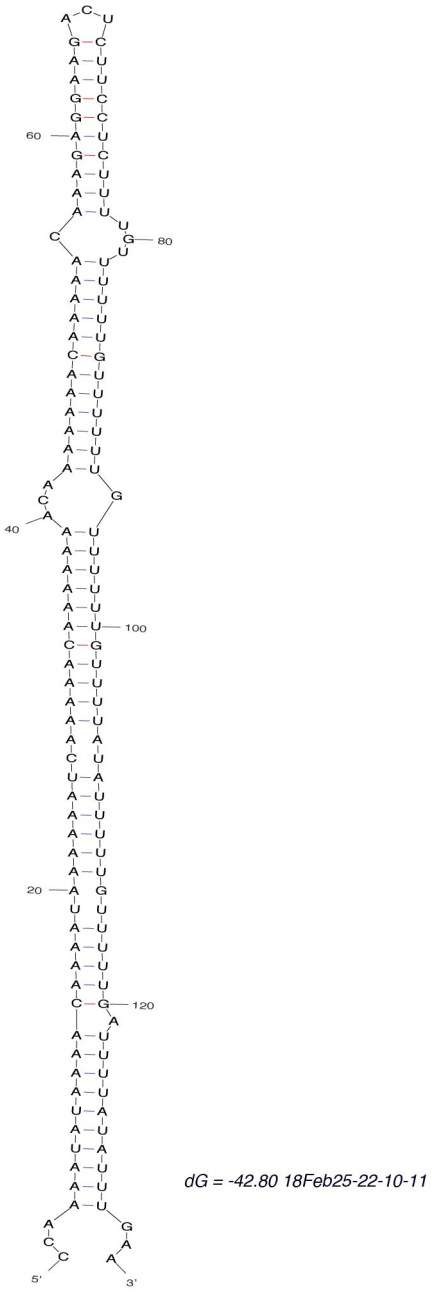

Fig. S4. Multiple alignment of the local sequences (putative endonuclease domain) of L-polymerase of LeNSRV2 and the recently discovered bipartite or tripartite phenui-like viruses associated with ticks and plants. The alignment was generated using MAFFT version 7 (Katoh and Standley, 2013) (http://mafft.cbrc.jp/alignment/server/), and conserved residues are shown in bold and highlighted.

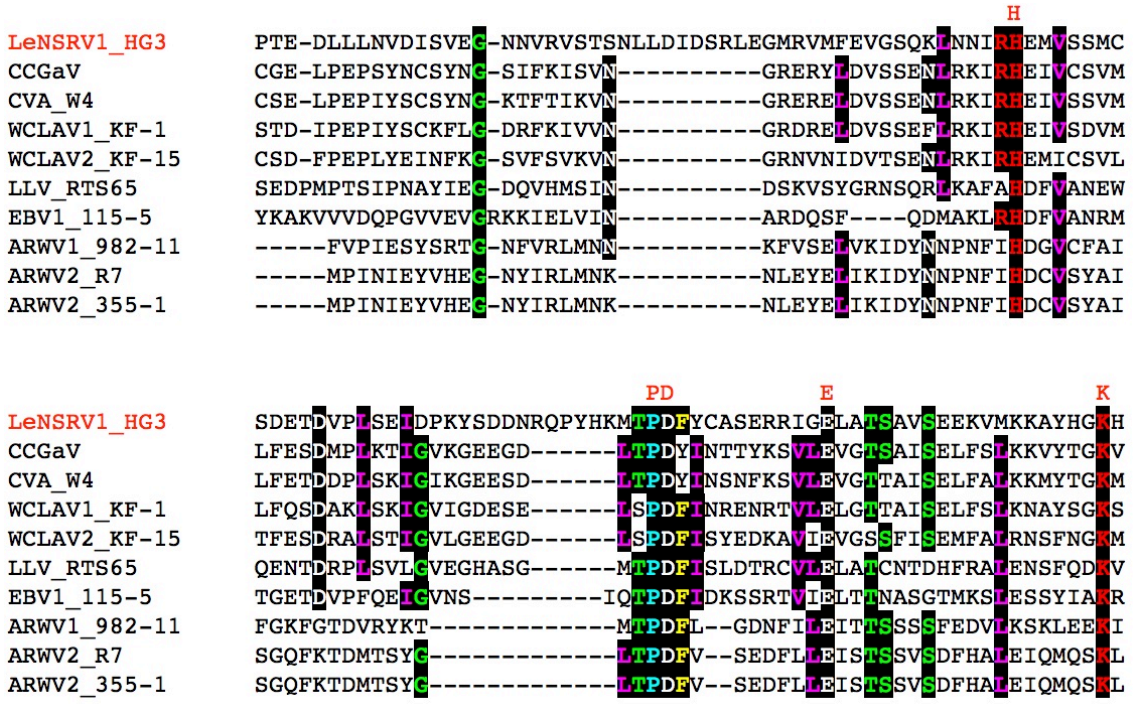

Fig. S5. Predicted stem loop in the intergenic region of the RNA2 positive strand of LeNSRV2, showing with a red box in the Fig 4B.

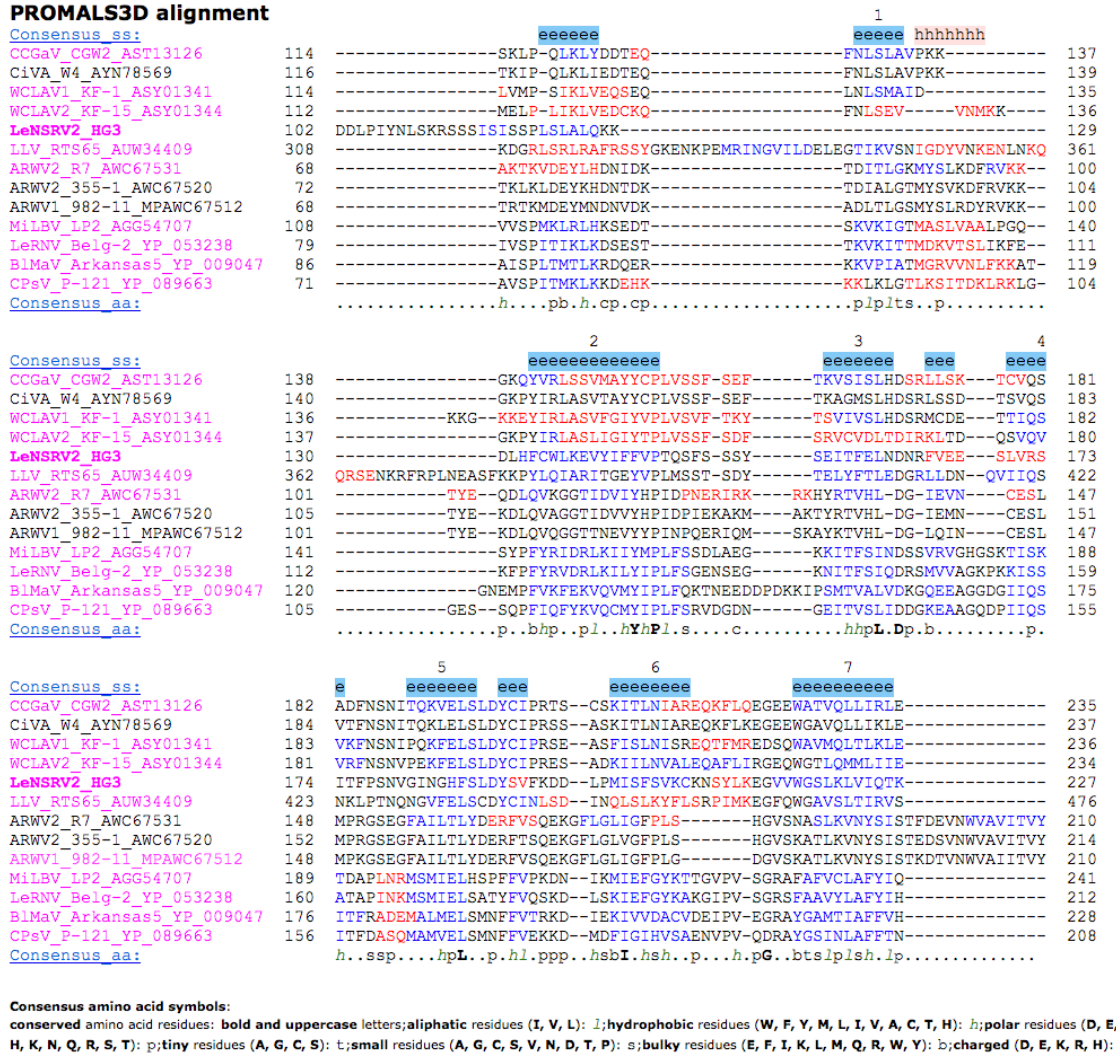

Fig. S6. Multiple alignment of the center region of movement proteins (MP, members of the 30K superfamily) from ophioviruses and MP-like-proteins from LeNSRV2 and its related phenui-like viruses. Virus names are followed by GenBank accession numbers. Each sequence is colored according to PSIPRED (Jones, D.T., 1999. Protein secondary structure prediction based on position-specific scoring matrices. Journal of Molecular Biology 292, 195-202) secondary structure predictions (red: alpha-helix, blue: beta-strand) within the PROMALS3D program. Consensus predicted secondary structure are indicated at the top with symbols, h (alpha-helix) and e (beta-strand), respectively. The highly conserved aspartic acid (D) is presented in an adjacent part of the number 3 beta-strand. Abbreviations for ophioviruses: CPsV, citrus psorosis virus; lettuce ring necrosis virus, LeRNV; blueberry mosaic associated virus, BlMaV; Mirafiori lettuce big-vein virus, MiLBVV.